University of
South-Eastern Norway

www.usn.no

FMH606-1 22V Master's Thesis 2022

Emission Free Construction Site-Thermal Overloading of the Charging System

Muhammad Akhlaq

Faculty of Technology, Natural sciences and Maritime Sciences
Campus Porsgrunn

Course: FMH606-1 22V Master's Thesis, 2022

Title: Emission Free Construction Site-Thermal Overloading of the Charging System

Number of pages: 78

Keywords: Emission Free, Thermal Overloading, Charging System, CCS-2, Temperature rise, DC Resistance, Overloading, Connector, Inlet, Thermal modeling

Student:	Muhammad Akhlaq
Supervisor:	Elin Fjeld
External partner:	**Skagerak Energi**

Summary:

In Norway, many municipalities set the target toward the emission-free construction site. Skagerak Energi also took a step toward this emission-free construction site by charging the construction machinery with the help of a mobile battery. To replace the typical diesel/petrol engine machinery with the electric battery fast charging of construction machinery batteries is most important. Charging Cable plays a critical role in the whole setup as it always carries a high current from ten to a hundred amperes of current. High currents put a lot of thermal stress on the cable and as a result, heat will damage the cable insulation aging materials. So, in this thesis, the thermal overloading of the Combined Charging System (CCS-2) cable is analyzed by doing the different tests on the DC part of the cable such as the DC Resistance Test, Temperature rise test on the rated current of the cable, and Overloading test in the University high Current lab.

DC resistance test helps to check the quality, Power loss in the cable, and temperature rise of the cable. As higher resistance will generate more heat in the cable. The temperature rise test evaluates the performance of the cable and checks cable does not overheat during operation. As every construction site has different construction machinery so overloading tests are performed to check the overloading capacity and how much time it will take to cross the IEC temperature limit when 20℃ is the ambient temperature. Based on the results charging model is proposed to avoid the thermal overloading of the charging system. On the rated current 250A the CCS-2 cable will take approximately 3 hours to get the steady-state temperature without getting the overheated. It means the rated current does not affect the thermal characteristics of the cable and charges the batteries on the construction site without crossing the IEC limit. The CCS-2 cable will take 23 minutes to cross the IEC temperature limits in the case of overloading when supplying 350A and in the case of 300A, the cable can be overloaded for 45 minutes when the ambient temperature on the construction site is 20℃. The DC resistance of the cable contact is $84\mu\Omega$. A thermal model of the cable using the electrical analogy would help to determine the temperature rise in every component and when the temperature becomes critical for the charging cable.

Preface

The Master Thesis titled “Emission Free Construction Sites-Thermal Overloading of the Charging System” was done by the master’s students from electrical power engineering as a part of FMH606 Master's Thesis, 2022 at the University of South-Eastern Norway (USN), Porsgrunn.

The purpose of the report is to discuss the overview of battery containers for a construction site, the charging and discharging process, and the thermal overloading of the charging system. The project is a part of Skagerak Energi’s pilot project “Mobile energy to emission-free construction sites.”

I would like to express my sincere gratitude to my supervisor Elin Fjeld for her guidance, encouragement, and support throughout this thesis. His effective and supportive dialog, useful advice, structural guidance, and motivating me to work towards the thesis goals. I would also like to thank you Mohammad Yassin for helping and guiding me during the different connections of cable as well as during the performing of different tests. I would also like to thank Skagerak Energi for providing me Combined Charging System (CSS-2) cable to examine the thermal overloading of the charging cable. At last, I would thank Thomas Øyvang for arranging a different presentation with the Skagerak Energi staff.

Porsgrunn, 18-May-2022

Muhammad Akhlaq

Nomenclature

CCS2—Combined Charging system Type 2

EVSE—Electricity Vehicle Supply Equipment

GHG—Green House Gas

ICEV—Internal Combustion Engine Vehicle

PEI—Power Electronic Interface

IPT—Inductive Power Transfer

ACEA—European Automobile Manufacturers' Association (ACEA)

SAE—Society of Automotive Engineers

AC—Alternating Current

DC—Direct Current

IEC— International Electrotechnical Commission

EV—Electric Vehicle

NEMA—National Electrical Manufacturers Association

PWM—Pulse Width Modulation

PLC—Power Line Communications

Contents

List of Figures

List of Tables

1 Introduction

1.1 Background

Over the last many years construction industry is rapidly growing due to the increase in population but this hurts the environment in the form of CO_2. According to the European Commission, the building sector accounted for 40% of energy use and 36% of CO2 emissions in Europe. Specifically, the construction sector in Norway is responsible for 1.2% of emissions of greenhouse gas or approximately 660,000 tCO2.[1] Around 5% of emissions come from the heating and drying of structures during construction, with the remaining 95% coming from transportation and machinery.[2] All construction sites release various gases like methane, Carbon dioxide, and other waste pollutants which harm the environment and also cause global warming. Air pollution, water usage, land usage, energy consumption, natural resource consumption, and waste generation are all detrimental effects of the construction sector[3].

Hence measures should be taken to reduce these emissions from the construction sites and make the environment ecofriendly. In this regard, Oslo Municipality has set a goal to reduce direct greenhouse gas emissions by 95% by 2030 and 52% by 2023, compared to 2009[4] One way to reduce these emissions is to use electrically driven construction machines. But this is not recommended use because electric grid stations cannot install at every place and the use of an exciting grid only for construction sites is also not a good option. So Mobile battery is the best option for the grid connections as well as for the power-up electric construction machines at sites.

A fossil-free construction site is one where no fossil fuels are used in any of the on-site construction activities. Bioenergy and biofuels, as well as alternative renewable energy sources such as electricity and hydrogen, are frequently used to replace fossil fuels. An emission-free construction site produces no greenhouse gas (GHG) emissions directly or indirectly because of its building activity. Now the result is that all the municipalities of Norway moving towards emission-free construction rapidly despite some barriers and challenges. Skagerak Energi also takes a step toward the emission-free construction site and starts the master project by the name “Mobile energy to the emission-free construction activities”. One part of the project about the Voltage Stability Simulation of High-capacity Charging Platform for Emission Free Construction Sites was done last year by the master students of USN as a semester project.[5] The fast DC charging cables are used to charge the construction machinery to reduce time and also due to high-power charging systems, which allow machinery to be recharged in a time comparable to that of a normal internal combustion engine vehicle (ICEV).

Fast charger Level 3 which can deliver up to 400A current[6]. Heat generation is a severe problem with such a high current. The collection of heat accelerates the aging of cable insulation and reduces the cable's lifespan. So thermal characteristics of the cable are of utmost importance for the long life and proper function of the cable.

EV charging cables are designed to carry a specific current during the charging. The EV cable will be overloaded when more than the rated current pass through the cables. As a result of overloading the cables get heated quickly, can melt, and start a fire after some time. There are different types of machinery involved on the construction site with different power ratings. So due to different types of machinery, there is the possibility of overloading the charging cable for a short interval of time of charging the batteries. Thermal overloading of the CCS-2 cables is important to prevent the overheating and long life span of the cable. In this thesis, thermal overloading of the charging system is discussed, and do some tests to identify the characteristics of the Combined Charging System(CCS-2).

1.2 Previous Work

The growing demand of fast electric vehicle charging needs attention to specify the loadability of the cables in a steady-state and short-term loading of cables. The cable capacity is limited due to the temperature rise that has a big impact on the cable insulations, and life span. Although there are many studies on thermal assessment of cables [7] and thermal analysis of the power cables in air.[8],[9]

In 2019 Oslo municipality set the target of moving from fossil fuel to electrified equipment on the construction site. For that, they build out the important electricity infrastructure, cooperated with the construction industry, and released funding for electric construction on site. As a result of these measures first, a zero-emission construction site began operation using the electrified equipment in September 2019. The project was to improve two streets of Oslo downtown. All the equipment used an electric battery to charge the machinery.[10]

In this master project from Skagerak Energi batteries will be charged in charging platforms that are connected to the grid and then these mobile batteries will charge the construction machinery on the construction site. One part of the master project which is related to the effect of load on the voltage stability of the grid station and the impact of load on other customers is discussed in the "Voltage Stability Simulation of High-capacity Charging Platform for Emission Free Construction Sites "by the USN master students as semester project [5].In that project, three grid stations are selected based on power, locations, and map the energy demand from the grid station to the electric construction machines.

1.3 Skagerak Energi Work

Skagerak Energi has gained funding from Enova for a research project where mobile battery containers are used in the electrification of construction sites. The idea is to charge batteries at a location where the grid has high capacity. Fully charged batteries are then driven from the charging station to the relevant construction site to supply battery-powered construction machines. Together with Skagerak Energi, Skagerak has procured a battery container with this new technology of the size of 576 kWh capacity *[5]*. Figure 1-1 shows the overview of the emission-free construction site from the grid to the building location. Skagerak provides the CCS-2 cables to investigate the thermal overloading of the charging system which is the main goal of this thesis.

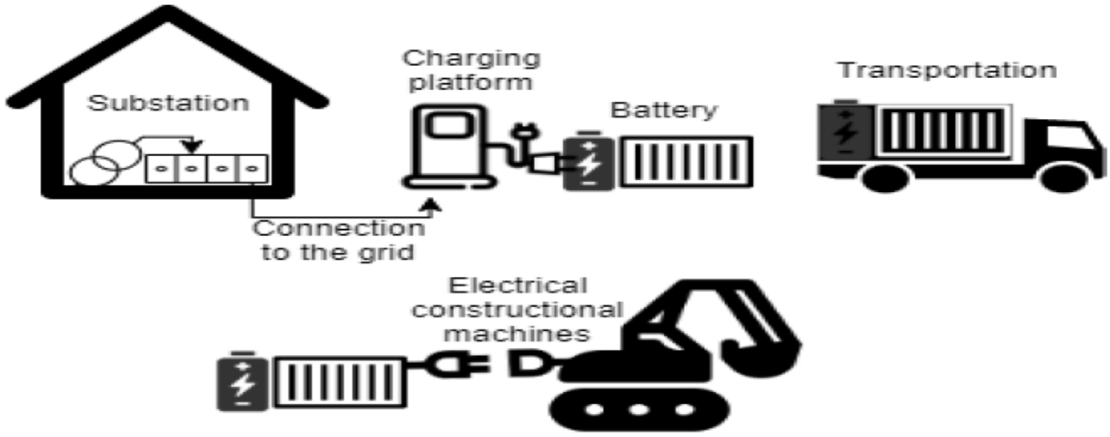

Figure 1-1: An overview of battery container from construction site to grid connection[5]

1.4 Objectives

As the batteries will be charged by the fast-charging cable CCS-2 on the charging station which is connected to the grid, the effect of fast charging on the cable must be studied. The charging cable is one of the most important components of an EVSE, and it plays a valuable and meaningful purpose in charging. The current carried by EV charging cables can range from tens to hundreds of amps. Such a high current can cause of producing heat in the cable conductor which damages the cable insulation and reduces the life span of the cable. The temperature of the cable conductor will be measured on the rated current and more than the rated current in case of thermal overloading. The other important goal is to identify the limiting factor of the cable when it comes to thermal overloading. The primary objective for these goals is described below, and the task description for this thesis is described in Appendix.

- Make an overview of the charging system.
- Identify what equipment is the limiting factor when it comes to thermal overloading.
- Study theory regarding thermal dimensioning of relevant equipment.
- Search the literature for studies on temporary overloading of relevant equipment.
- Investigate what temperature limits apply.
- Make a test set-up in the high current laboratory for thermal testing of charging cables.
- Use the tests to make an initial, simplified thermal model of the charging cables.

1.5 Limitation

This master thesis is a part of Skagerak Energi's pilot project "Mobile energy to emission-free construction sites."All the tests are conducted in the lab but consider the practical situation.CCS-2 charging cable is the test object and only the DC part of the cable is considered for the thermal overloading of the cables. So this master thesis has some simplifications or limitations.

- Three main tests are performed in the lab to target the main goal of the thesis. DC Resistance, Temperature rise test, Overloading Test.
- During these tests, the inlet port is connected to the power supply and the connector part is shorted. The only reason is to pass the current through the cable. But this is not true in practical. The inlet part is placed inside the vehicle and the connector is in the open air with the charging station. In this thesis, both the inlet and connector are placed outside in the open air.
- To measure the DC resistance of different parts of the cable only 50A DC is applied. Due to the lack of frequency, no proximity or skin effect occurs across the conductor when DC is supplied. Instead of bulk resistance, contact resistance and resistance per unit length are important. Then compared the expected value with the measured value to check the quality of the cable and also help in temperature rise.
- During the temperature rise test make sure the contact temperature does not exceed ambient temperature +80℃. If the temperature crosses this limit, then the current from the power supply is reduced to avoid any serious problems.
- Two overloading currents tests on the CCS-2 charging cable. During the tests make sure that the temperature of the cables does not cross the ambient temperature of the cable +80℃ and note down the temperature, and time parameters for the thermal model of the charging cables.

2 Emission Free Construction Site

This chapter highlights the emission-free construction site and focuses on the charging station as well as the charging platform because the CSS-2 cable is used to charge the construction machinery and also charge the batteries.

The figure shows 2-1 the block diagram of the different components involved in the emission-free construction sites. First, start to form the construction site and map the energy required on the construction site as well as also figure out the compatible components for the battery containers. Construction is the process of building together infrastructure utilizing a detailed plan and various resources. A construction site can be anything like a residential/Commercial building or highway construction. Then Charging station is the most important component because it plays a vital role between the construction site and the mobile battery. The second most important component is the charging platform because on this platform the batteries are charged from the grid.

When the fully charged batteries are transported to the construction site then a proper charging platform is required which is compatible with construction machinery. The charging ports could be included in the container or connected to an external distribution board. Using the outlets as an external distribution board may be advantageous to ensure that the container has the most battery capacity possible. Simultaneously, it would be simpler to adjust the number and type of outlets to match the number and kind of plugs on each construction site. One fully charged battery can charge the two construction machines according to the report [5]. The charging system should have enough space to charge the machines and manages the cable to be safe and secure. The CCS-2 cable is used on the charging station as it can provide power at up to 350 kW[11]. The CCS type-2 charging cable is shown in figures 2-2. It has a high power charging capacity leading to fast charging and these cables are widely used for charging electric vehicles in Europe.

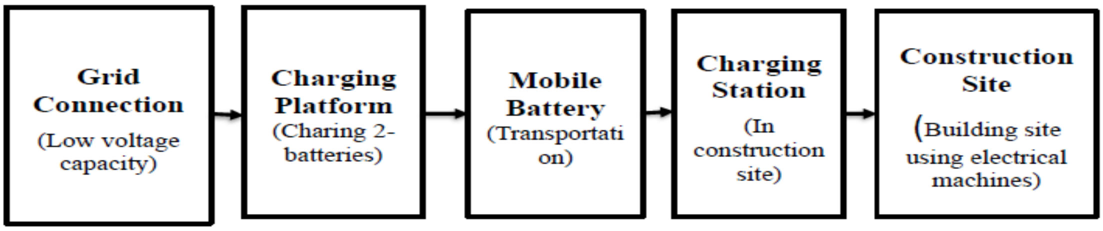

Figure 2-1:Block diagram of overall process of emission free construction site[5]

The CSS-2 cable is also used to charge the batteries from the grid stations. To avoid the voltage instability at the grid make sure the grid has enough power and other customers will not disturb by the charging. The charging platform is designed in such a way that multiple batteries can be charged at the same time. It's important to have a mechanism that distributes current equally so that grid can charge at least one battery while not surpassing the grid's power cut. In such a case a fast charging cable CSS-2 is perfect to use on the charging platform to charge the batteries due to its fast charging ability. The charging platform takes 1 MW of grid energy to charge two mobile batteries[5]. When the charging platform charge two batteries, the mechanism limits the charging power to 500 kW per battery,[5] whereas one battery needs 576 kW for charging. The CCS type-2 cable is suited for charging the batteries, and at least two cables are enough to charge a single battery. The charging station and platform are interesting objects for this thesis as CSS-2 charging cables are used to charge construction machinery from the Mobile batteries and batteries from the grid. So in these two components, the charging cable plays important an role.

According to the project descriptions the batteries are charged during the lunch break for 30 minutes. So for such a short interval of time, the cables can be overloaded but important thing is that make sure the temperature limits must be kept within the limits during the short interval of overloading. As this is fast charging and cables carry high currents. So based on the temperature calculations a thermal model is proposed to predict the temperature of the cable conductor. To check the thermal overloading of the cables some tests are planned to do. For that, a physical setup is made in the High current lab at USN.

Figure 2-2:CCS-2 inlet[12]

3 EV Charger

An EV charger is a device that converts alternating current energy into direct current to recharge the energy storage device (i.e., the battery) and provide energy to the other electrical vehicle systems for proper functioning. To charge the electric vehicle from the charging station three functions must be accomplished. Of three functions one is mechanical whereas the other two are electrical functions. The mechanical function is the physical function between electric vehicles and electric vehicle supply equipment. The first electrical function towards the charging is the rectification process and the second one is checking the supply voltage according to the battery acceptance level. [13]

The charger has three roles.

i. Charge the battery from the charging point (Charging)

ii. Increasing the charging rate to its maximum potential (Stabilizing)

iii. Know when to stop charging (Terminating)

The charger control unit, charging cable, and vehicle control unit are the main parts of the EV charger system[13]. Figure 3-1 is the block diagram of the EV charger.

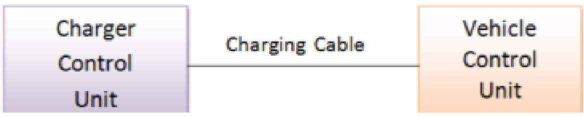

Figure 3-1:Main part of EV charger[13]

There are two types of EV chargers Onboard and Off board. In the case of Onboard EV, users can charge the vehicle any time when they want. The vehicle has a power source and charging point inside. The main disadvantage related to the onboard charger is the limited option of power and due to this option, only a level 1 charging is available. Cost, weight, and space issues are the main reason which bound the power to level 1[14]. But such kinds of issues can be solved by the use of a resonant circuit. As shown in figure 3.2. Nowadays Onboard chargers are common in the market.

On the other hand Off-board charger, and fast-charging stations are also demanding and gaining more popularity day by day. DC charging stations have some good advantages such it reduced the EV weight, it can charge at a high level, and also enhanced battery management systems e.g heating problems and appropriate communication between utility companies and business site owners to create charging conditions that will lead to improved contractual chances.[14] The advantages and issues related to the onboard and off-board charger are explained in table 3.1.

Table 3-1:Adavantage and issue of on-board and off-board[14]

Charger	Advantage and Issues
On-Board Charger	Transfer of energy (kW) is less.
	The issue of battery heating.

	The weight of an electric vehicle has been increased.
	Slow charging
	To handle battery management systems, onboard rectification is used
	Because of the Electric Vehicle architecture, size and weight are limited.
	In terms of charger interface, the protocols for communication aren't up to industry standards.
Off-Board Charger	Increased energy transfer (kW)
	Charge with more power.
	Battery heating must be addressed.
	The EV's weight has been removed.
	BMS systems are much better.
	Increased complications and costs
	Adding a BMS to a charging station is expensive and time-consuming.
	Offboard BMS does not allow for the detection of defective battery pack cells.

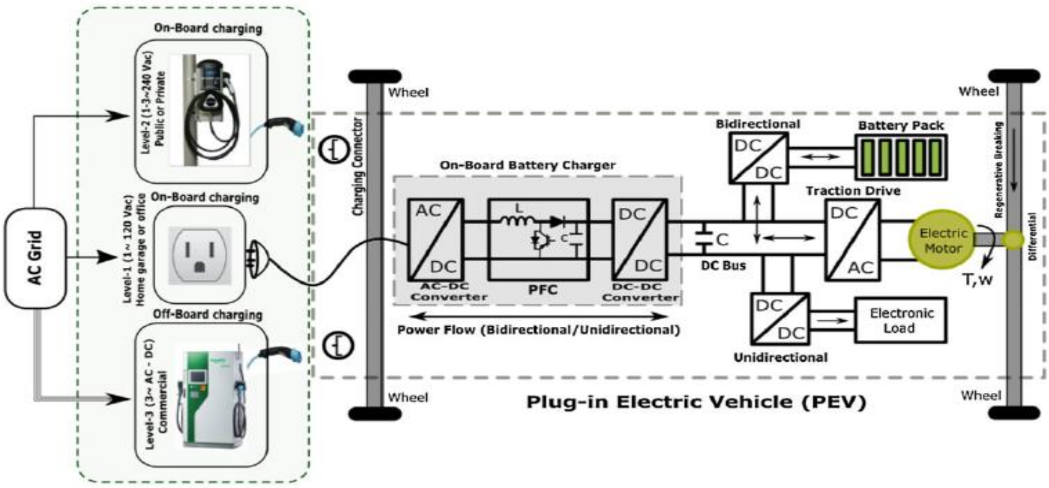

Figure 3-2:Infrastructure for electric vehicles (EVs), including charging power levels and onboard/offboard charging systems[14]

3.1 EV charging Techniques and standards:

The challenging issue with the use of EVs is their charging. The charging means the electric power from the grid is at an acceptable level and injected into the battery. The charger power level and battery are both important for the charging times. The main issue is the battery's limited life and charging time.[15] Figure 3-3 shows the different charging techniques.

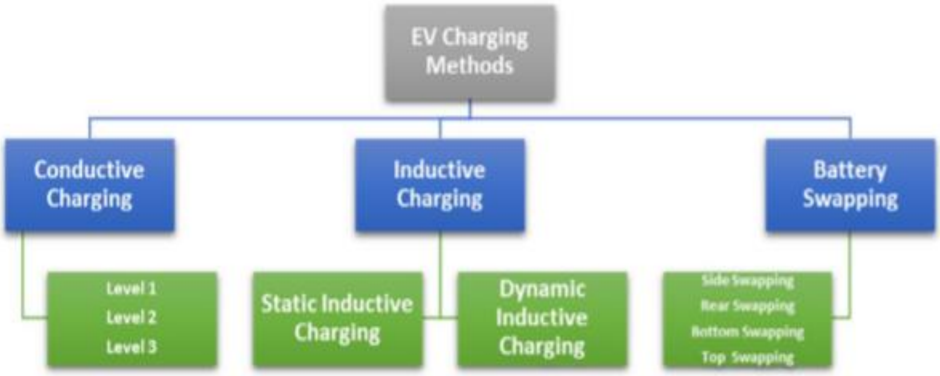

Figure 3-3:Various EV charging Methods[15]

3.1.1 EV charging Method:

Three methods are used for charging; the Conductive charging method, Inductive charging method, and battery swapping method[15].

3.1.1.1 Conductive Charging:

Conductive charging means physical contact between the supply network and the vehicle. In other words, charging allow direct connection between the charger and vehicle. It is divided into onboard and off-board which consists of a rectifier and converter. On-board chargers have inside whereas off-boards have outside rectifiers and a battery regulation system. [15].The physical connection between the charger and the car prevents contact at higher potential differences. A fast charger can be damaged due to the high power level of charging.

3.1.1.1.1 The Charging Level:

The charging level explains the power level of the charging outlet.

Level 1 charging:

This is the lowest level of charging. In USA level, 1 means a standard 120V/15A single-phase grounded outlet such as NEMA 5-15R.[16] Level 1 does not need additional infrastructure for home and office sites. Late at night, low off-peak rates are likely to be available. It's an EV charging method that involves the most common grounded electrical socket and a suitable cable setup to extend AC power from the electric supply to an onboard charger. [16]

Charging Level 2:

Level 2 charging is called the fast AC charging either 7kW (32A single phase)or 21kW (three phases)level. In this method, AC power extends from the electric supply to an onboard charger from a special EVSE.[16]

Charging Level 3:

Level 3 uses the special direct current supply equipment to charge the EV from a special off-board charger either in public or private. A conductive charging system helps to provide power from the off-board charger. Level 3 charging is referred to as "Fast DC charging," with a capacity of up to 50kW and a charging period of 20 minutes from empty to 80% full (the last 20% of DC charging takes a long time, hence DC charging is commonly measured up to 80%).[16] Figure 3-4 shows the AC level 3 charging system.

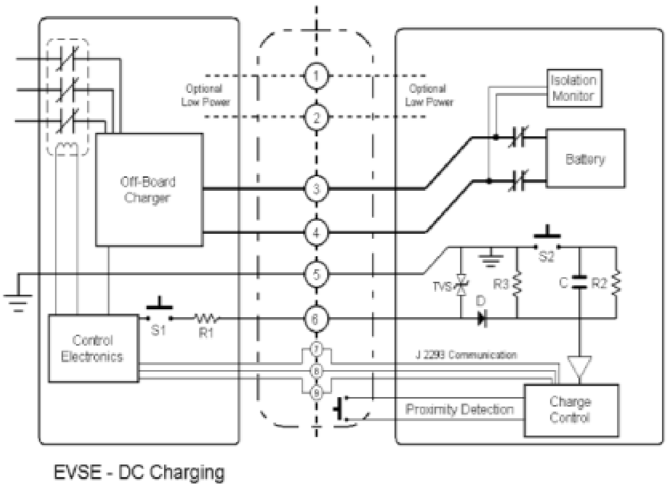

Figure 3-4:AC Level 3 System Configuration (SAE_J1772 Standard[16]

3.1.1.2 Inductive Charging:

There is no physical connection between the power supply and power electronic interface (PEI) in inductive charging or contactless charging. Inductive works on the principle of Inductive power transfer(IPT) principle, which transfers the power through the air to the load without making any physical connection. Additional advantages of IPT systems include stability, the removal of contactor wear from extensive usage, and heat cycling. The magnetic circuit contains the primary(AC side) and the secondary (Vehicle side).[17]

3.1.1.3 Battey Swapping:

Battery swapping is another option for charging the EV. When the energy in an electric vehicle is about to run out, it refers to the quick recovery of such energy through battery replacement. Electric vehicle customers just buy cars and rent batteries from service providers, decreasing ownership costs and solving the issue of long charging times. Battery swapping can be done in a variety of ways, depending on the placement of the battery in the vehicle and the robotic arm's application point.[15]

3.1.2 The EV charging Modes:

Recharging modes are divided as modes 1-4 in the international standard IEC 61851-1[18]

3.1.2.1 Mode 1:

A single-phase line that is not more than 250V AC or a three-phase that is not more than 480v AC is connected to charge the EV. The plugs and sockets with protective earth depend on the countries in which the charger is used. This charging method is the slowest, yet it may recharge a battery overnight, bringing it up to full capacity before dawn. This type of charging has a low effect on the grid in the shape of the load. Because no extra infrastructure is required, this recharging option is primarily employed at home and in the office[13][18]. Figure 3.5 explains charging mode 1.

Figure 3-5:EV charging Mode 1 and cable[19]

3.1.2.2 Mode 2:

Mode 2 has the same voltage level as mode 1 with the same plugs and sockets but the difference is only in mode 2 both vehicle intake and connector have the control pin. Because the control function is provided by an integrated control box with the additional function of a cable protection device. This form of recharging is mostly employed in private facilities[18].[13]. Figure 3.6 helps to understand mode 2.

Figure 3-6:EV charging mode 2 and cable[19]

3.1.2.3 Mode 3:

In Mode 3 EV connect with an AC power supply with the help of EVSE for charging with a maximum current of 63A. It has a control pilot function, as in mode 2, to control equipment that is permanently attached to the AC supply. In this mode 3 charging cable need a special connector with some control and signal pins. This recharging mode is common at public charging stations, and it's powered by three-phase AC power at 50/60 Hz. It's also known as a semi-fast charging solution because it can charge a battery in a few hours while the driver is at work or going about their daily routine[18][13]. Figure 3.7 shows mode 3.

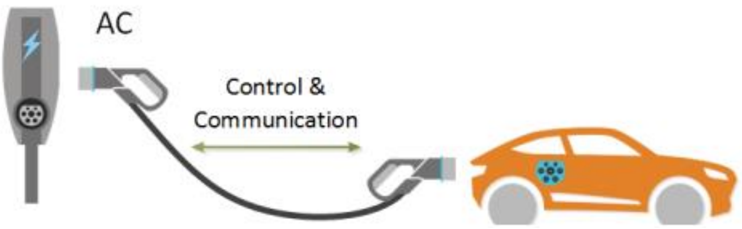

Figure 3-7:EV charging mode 3[19]

3.1.2.4 Mode 4:

In mode 4 charging station converts the AC to DC, and the socket ensures that only a compatible electric vehicle can be connected. The charging time for mode 4 is usually between 20 and 30 minutes. This charging mode could provide a recharge from 0 to 80 percent of the battery in 20-25 minutes by combining high power converters with the newest battery technologies (ultra-fast charging).[18][13].Figure 3.8 shows the EV charging mode 4.

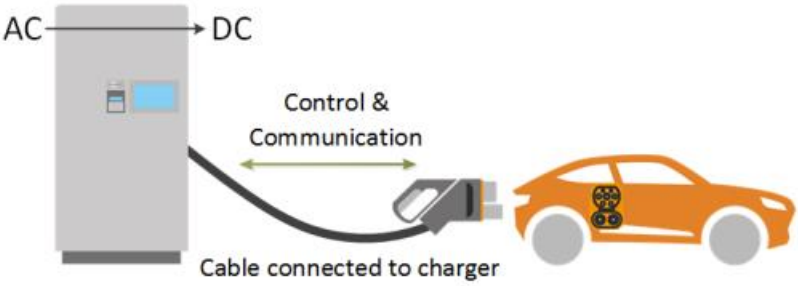

Figure 3-8:EV charging mode 4[19]

3.1.3 DC Fast Charging:

The lack of charging stations and long charging are the two main problems with the adoption of the electric vehicle. The level-3 charging idea, which is also called Fast-Charging, primarily addresses these problems[20]. Level 3 charging should use an off-board AC/DC and/or DC/DC conversion system that is connected directly to the EV battery pack. CHAdeMO, combined charging system (CCS), and Tesla Supercharger are the three major charger technologies now in use, notably for fast charging. Table 3-1 shows the specification of each charging standard.

Table 3-2:DC charging standard[20]

Properties	CHAdeMO	Combo 1(CCS)	Combo 2(CCS)	Tesla Supercharger
	DC charging			
Max.Voltge(V)	500	600	1000	480
Max.Current(A)	125	150	250	

Connector	CHAdeMO	Combo 1(IEC 62196-3/SAE J1772)	Combo 2(IEC 62196-3/SAE J1772)	Special
Max. Power(kW)	50	90	170	120
	AC charging			
Voltage(V)	--	250	400(3 phase) 230(1 phase)	
Current(A)	--	32	63(3 phase) 70(1 phase)	
Max. Power(kW)	--	13	44	
Charging Signal	CAN	PLC		
Charging Protocol	CHAdeMO	Home Plug Green Phys		Special

A high-power CHAdeMO charger is capable of charging at 100 kW continuous power and 150–200 kW peak power (350 A, 500 V). Furthermore, in 2020, a higher-power CHAdeMO was designed that can charge at 350–400 kW (350–400 A, 1 kV)[21].[20]
CCS standards (Combo 1 and 2) can use both AC and DC charging, including level-1 and level-2 charging. With the help of CCS easier to charge both AC and DC vehicles using a single charging outlet. CCS can support AC charging at a maximum rate of 43 kW and DC charging at a maximum rate of 200 kW, with the potential to increase to 350 kW in the future.[20]

3.2 Combined Charging System (CCS-1 and CCS-2)

It is now impossible to have a single type of connector throughout the world. This is because several electrical grid systems exist around the world; for example, Japan and North America use a 1-phase connector on their 120/240 V grid (type 1), while China, Europe, and the rest of the world use a connector with 1-phase 230 V and 3-phase 400 V grid access (type 2). The Combined Charging System, or CCS, is a concept established by the SAE in the United States and the European Automobile Manufacturers' Association (ACEA) to add DC wires to current AC connector types, resulting in a single "global envelope" that fits all DC charging stations. Two extra connectors are added to the bottom of Type 1 or Type 2 vehicle inlets and charging plugs for Combined Charging System (CCS).[22] In general, Combo 1 style vehicle inlets are used in North America, while Combo 2 style vehicle inlets are used in the rest of the world. : Plugs and Inlets for CCS Types 1 and 2.[23]

Figure 3-9:Plugs and Inlets for CCS Types 1 and 2[23]

The main aspects of the combined charging system include the following.

- AC Charging
    1. With the electrical interface standards for power transmission, which incorporates IEC 61851-1-compliant safety-related signaling for AC charging
    2. In Europe, with a Type 2 connector that meets the international IEC 62196-2 standard.[23]
- DC Charging:
    1. The IEC 61851-23-compliant electrical interface protocol for power transmission incorporates safety-related signals for DC charging.
    2. In Europe, the Combo 2 connector, which complies with the international IEC 62196-3 standard, is used.[23]
- Based on the international standard ISO/IEC 15118 and the German DIN SPEC 70121, the communication interface between the electric car and the charging point.[22]

Charging Type:
AC and DC charging is supported by the CCS. There are two charging control methods for AC:

- PWM-based basic signaling
- PLC-based high-level communication

Charging through AC One or both of the charging process control techniques are supported by CCS.
CCS for DC charging support only

- PLC-based high-level communication

is required for the external DC charger's control.[23].

Table 3-3:Advantage of CCS[24]

Advantage	Description

Safe Charging	During the charging process or before all essential operations, such as payment, an electromechanical actuator locking mechanism prevents the vehicle connector from being withdrawn. This ensures a high level of operational security.
Fast Charging	Due to the fast charging, it can charge up to 250A, which is larger than AC charging. Because AC charging provides only 32A.The vehicle connector's ergonomic handle design and low insertion and withdrawal forces ensure fast, convenient, and easy handling.
Intelligent Charging System	The signal and control contacts, CP and PP, are used for communication and control in both AC and DC charging modes.

3.2.1 Combined Charging System (CCS-2)

For daily charging applications in Europe, the CCS Type 2 is the best option to choose for charging. CCS-2 can charge the vehicle using both traditional AC and DC while on the road. The CCS-2 vehicle connector can handle up to 250 A of DC electricity.[24] It is put into the vehicle inlet with a little amount of force. Normally CCS-2 has two parts. One is the inlet part and the other one is the connector part. Normally the inlet part is placed inside the vehicle and the connector part is used to charge the vehicle from outside charging stations.

Advantage Of CCS-2:[24]

- CCS-2 can charge the electric vehicle with flexibility.
- Both options are available fast and slow charging in the garage.
- Temperature across the contact is continuously monitored and also has the actuator lock for safe charging.
- Single charging system for all of Europe and North America.

3.2.1.1 Temperature Monitoring

To protect the charging process, it is important to monitor the charging current and temperature. The PT-1000 sensors are used to detect overheating in the system, such as high temperatures or an overload across the cable. If the temperature across the contact crosses the limit then The charging station can then turn off the charging process or reduce the charging power. The temperature increase must not exceed 90°C, according to IEC 62196.[25]

3.2.1.2 Actuator Locking

The CCS Vehicle Inlets have an electromechanical locking actuator, which secures the Vehicle Connector and does not let it go anywhere during the charging process. The actuator bolt is made to deal with a lot of pull-out force[25].

4 Theory

In this chapter different concepts are explained which will help to complete the desired task later in the measurement and results.

4.1 Heat Generation in Cables

When cables carry a load current, heat is created. The temperature of the cable is proportional to the load current; as the load current increases, so the temperature of the cable also increases. The type of conductor in the cable, the types of current flow in the conductor, the nature of the load, insulation type, joints, and other factors all affect temperature rise.

4.1.1 Conductor loss

Conductor loss occurs when an electric current passes through the conductor producing a power loss. This is the main cause of heat sources in the conductor. Equation 4.1 shows the conductor loss.[26]

$$P=I^2R \tag{4.1}$$

Where:

P – Power which is converted from electrical energy

R –Resistance of the conductor

I—Current passing through the conductor

4.1.2 Electrical Resistance

The electrical resistance of a wire or circuit is a measurement of the resistance to electrical current flow. The resistance of a good electrical conductor, such as copper wire, will be very low. The bulk resistance is the material's resistance, whereas contact resistance is the resistance of the connection between two individual pieces. Figure 4.2 shows the bulk and figure 4.1 contact resistance of the cable. The total resistance can be found by summing bulk resistance and Contact resistance. As seen from the equation 4.2

$$R_{tot} = R_{Cont} + R_{Bulk} \tag{4.2}$$

Where:

$R_{Tot} = Total\ resistance\ of\ the\ cable$ [Ω]

$R_{Con} = Contact\ resistance$ [Ω]

$R_{Bulk} = Bulk\ Resistance\ of\ the\ cable$ [Ω]

4.1.3 Contact Resistance

Contact resistance is the resistance to current flow, due to surface conditions and other causes when contacts are touching one another (in the closed condition of the device). The conductors only touch a few places. The real contact area is much smaller than the apparent contact area. The contact resistance depends on the surface roughness to a great extent. The pressure holding the two surfaces together also influences the contact resistance. Figure 4-1 shows the contact resistance measurement probes.

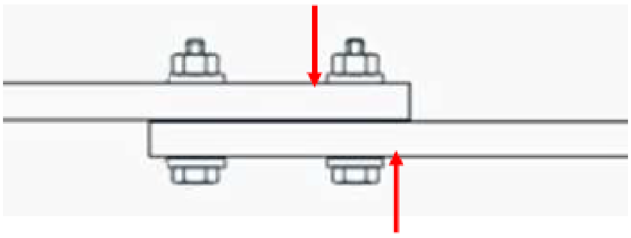

Figure 4-1:Contact resistance measurement[27]

4.1.4 Bulk Resistance

The Bulk resistance is depending on the length, area, and properties of the materials itself. Equation (4.3) explain the bulk resistance.[28] The property of the material is different for each material so the bulk resistance of each is different. Figure 4.2 shows the bulk resistance measurement probes.[27]

$$R_{bulk} = \rho \frac{L}{A} \tag{4.3}$$

Where:
$R_{Bulk} = Bulk\ Resistance$ (Ω)
$\rho = Resistivity\ of\ the\ material$ (Ωm)
$L = Length\ of\ the\ cable$ (cm)
$A = Cable\ cross\ section\ area$ (mm^2)

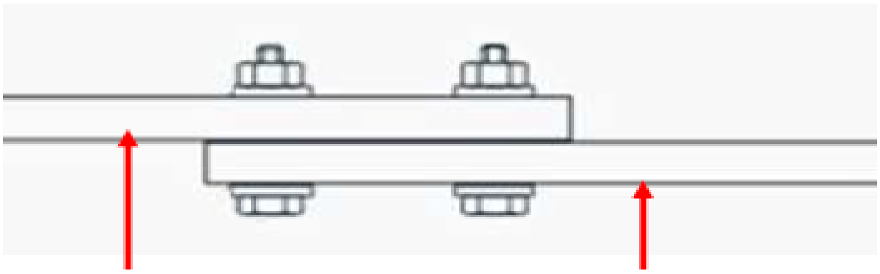

Figure 4-2:Bulk resistance measurement[27]

Table 4.1 shows the specific electric resistance and conductance of common electrical conducting materials at 20 degrees Celsius.[28].As temperature will rise in the conductor due to the heat loss. According to IEC-60277-1-1 the specific electric resistance for a temperature range of -50°C to 200°C can be found by using equation 4.4[28]

$$\rho_T=\rho_{20}[1+\alpha(T-20)] \tag{4.4}$$

α represents the temperature coefficient and T is the temperature at which the resistivity is calculated. The warm resistance of the conductor can be calculated by using the equation 4.5[29]

$$R_w = R_c(1 + \alpha(T_w - T_c)) \tag{4.5}$$

Where:

R_w –The warm resistance

R_C –The cold resistance

T_w—Warm temperature

T_C—Cold Temperature

Table 4-1: Electrical properties for different conducting materials at 20 ℃.[28]

Conductor	**resistivity ρ [Ωm]**	**Conductivity χ [$m/mm^2\Omega$]**	**Temperature coefficient α [K^{-1}]**	**Density [g/cm^3]**
Copper	$1.68 \cdot 10^{-8}$	$5.96 \cdot 10^{7}$	$4.04 \cdot 10^{-3}$	8.96
Aluminium	$2.65 \cdot 10^{-8}$	$3.77 \cdot 10^{7}$	$3.9 \cdot 10^{-3}$	2.7
Silver	$1.59 \cdot 10^{-8}$	$6.3 \cdot 10^{7}$	$3.8 \cdot 10^{-3}$	10.49
Nickle	$6.99 \cdot 10^{-8}$	$1.43 \cdot 10^{7}$	$6 \cdot 10^{-3}$	8.908
Iron	$9.7 \cdot 10^{-8}$	10^{7}	$5 \cdot 10^{-3}$	7.874

4.1.5 AC Resistance or DC Resistance of the Cable

When the DC passes through the conductor the entire area of the conductor is utilized whereas if the conductor carries an AC, the current is not uniformly distributed throughout the conductor and the current pass along the surface of the conductor. This is due to two independent effects known as the Skin effect and the Proximity effect. Due to this effect, the DC resistance of the cable is always high than the AC resistance. As DC & AC resistance of the cable is important for the selection of the conductor and helpful for the calculation of line loss of the cable. So, this is the reason why DC resistance is preferred over AC resistance.

4.1.6 Measuring the Contact Resistance

There will be an error in the measurement if an ohmmeter is used to measure the contact resistance of the cable because it measures the resistance of all the loop including ohmmeter wires with object resistance. Figure 4.3 explains the resistance measure when using the ohmmeter. So, this is not a good way to measure the resistance of the contact.4 wire method is used to overcome this problem.

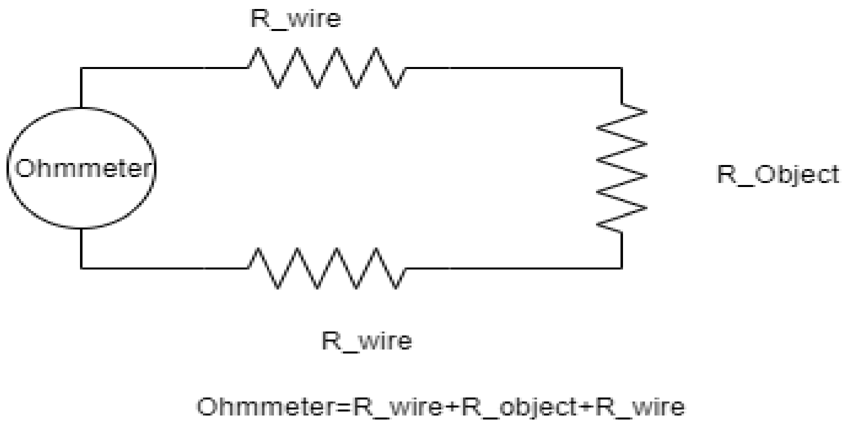

Figure 4-3:DC resistance using ohmmeter

The four-wire method is used for the contact resistance as the four-wire method eliminates the inherent resistance of the lead wires connecting the measuring instrument to the component being measured. It allows for precise measurements of resistance values smaller than 0.1Ω. When testing cables designed to carry large currents, precise low-value resistance measurements become important.

Apply the test current and measure the voltage drops across the cable for the resistance of the cables. Figure 4.4 shows the 4 wire method.

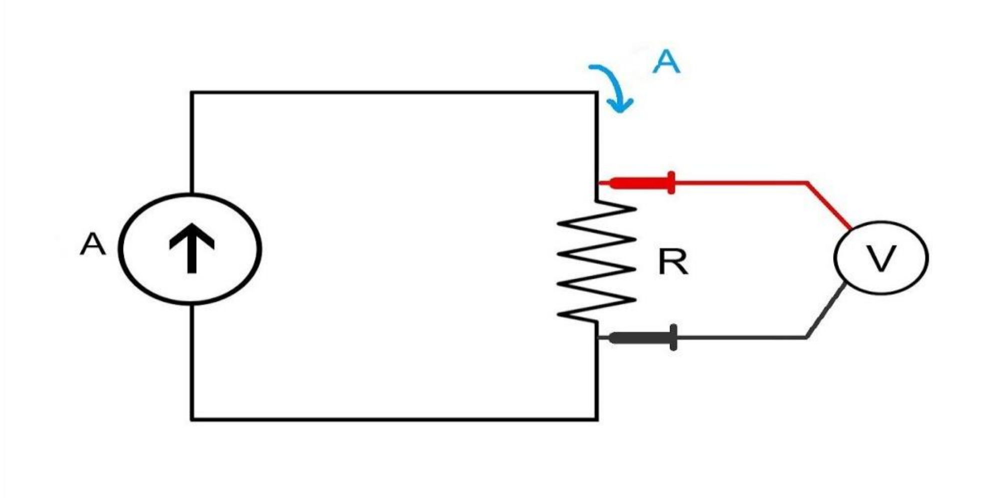

Figure 4-4:4-wire method[30]

by Ohm's law

$$V = IR \tag{4.6}$$

$$R = {}^{V}/_{I} \tag{4.7}$$

Where

$R = Resistance$ (Ω)

$V = Voltage\ drop$ (V)

$I = Current$ (A)

The 4-wire method is very practical. But there is a problem when doing the measurement and placing the probes too close or too far away from the contact. Especially in this test when we place the probes too far away then the bulk resistance will be included in the contact resistance. The longer the distance is between the probes, the more bulk is included which results in a higher bulk resistance included and the total resistance would be higher than intended. It is shown in Figure 4.2.

4.2 Skin Effect

When an alternating current pass through the conductor, the outer surface of the conductor always carries high current than the inner surface of the conductor. This effect is called the skin effect and it mainly depends on the high frequency of the conductor. Figure 4.5 shows that no current flows in the center of the conductor and all charges pass along the outer surface.

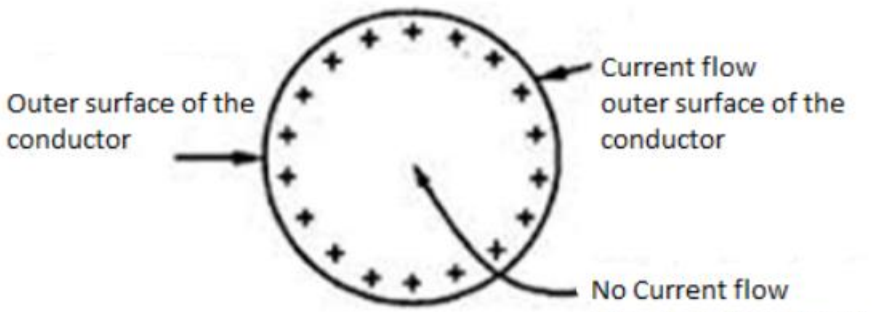

Figure 4-5:Skin effect[31]

The skin depth is a distance beyond the conductor's surface where the current density drops to $\frac{1}{e} \approx 37\%$ of its value. The skin depth formula is explained in equations 4.8[32]

$$\delta = \sqrt{\frac{2\rho}{\mu\omega}} = \sqrt{\frac{\rho}{\mu_r \mu_o \pi f}} \tag{4.8}$$

Where:

δ −specific electrical resistance

μ −permeability of the conductor

ω −angular frequency of the current

μ_r −relative permeability

μ_o −magnetic permeability in vacuum

f −frequency of the current

The frequency of the current changes the skin depth. Higher frequency produces lower skin depth. Skin depth is dependent on the conducting materials as shown in figure 4.6. The red lines show the 50 Hz frequency. In figure 4.6 the skin depth of the aluminum conductor is more than the copper due to the high resistance of aluminum at the same permeability. Comparing the iron and steel with approximately the same electric resistance shows that steel's skin depth is greater than iron's because iron is more magnetic and thus has greater relative permeability. For rated currents of 2.5 kA and higher, the skin depth can affect the effective cross-section of conductors, and a hollow conductor can be utilized to reduce the skin impact.[32]

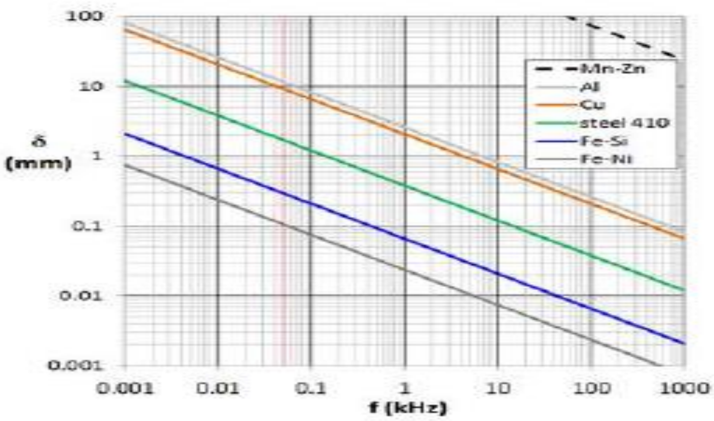

Figure 4-6:Skin depth of conductor materials for different frequencies at room temperature.[32]

4.3 Proximity Effect

A fluctuating magnetic field causes an eddy current in the surrounding conductor as a loop or coiled-coil of the wire as ac power passes through the conductor. Due to current distribution over the cross-section of a conductor in which current flows in the same directions, this leads to high current density in nearby loops. This effect is called the proximity effect. Figure 4.7 shows the proximity effect and where d is the distance between the conductors.[31]

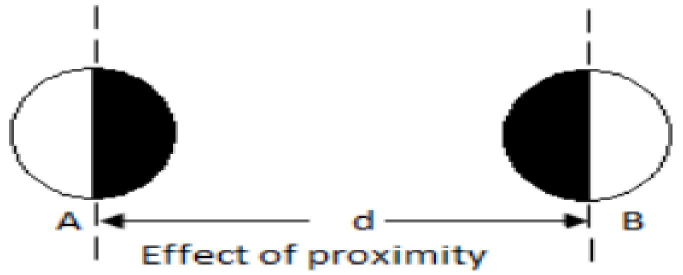

Figure 4-7:Proximity effect[31]

The electromagnetic field of the conductors interacts with others when multiple conductors are placed close together. The current in each conductor is distributed in such a way that the current density is concentrated on one side of the conductors and produces the eddy currents in the conductors. In addition to the skin impact, the proximity effect reduces the effective cross-sectional area. The proximity effect, like the skin effect, gets larger with frequency. The proximity effect reduces as the distance between parallel conductors increases, becoming inconsequential when the distance between two cables in two adjacent circuits is at least 8 times the cable's outside diameter.[8][32]

4.4 Induced Loss

Heat is produced in the hysteresis when a magnetic field changes the directional orientation in the ferromagnetic structure and as a result heat energy is lost. These induced losses are also called iron losses as the iron is highly ferromagnetic. Total iron loss can be calculated by the addition of then eddy and hysteresis loss.[32]

The area of the eddy current loop, the magnetic field strength, and the rate of change of magnetic flux are all proportional to the power loss. The conductor material's resistivity is inversely proportional to the magnitude of the current. According to Faraday's law.[33]

$$V_{ind} = -\frac{d\phi_m}{dt} = -\frac{d(\overrightarrow{B}.\overrightarrow{A})}{dt} \tag{4.9}$$

Where ϕ_m is magnetic flux, B is the magnetic field and A is the size of the loop. So power loss is explained in equation 4.10 [33]

$$P_{ind} = V_{ind}P_{ind} = \frac{V^2{}_{ind}}{R} \tag{4.10}$$

4.5 Thermal Time Constant

The thermal time constant is an important factor since it shows how long equipment can be overloaded without overheating. The heat generated inside conductors is balanced by two components, according to the law of conservation of energy.

- Heat stored inside the conductor (P_{stored})

- Heat losses into the surroundings ($P_{dissipated}$)

Input power which is changed into heat in the conductors is:

$$P_{in} = R \times I^2 \tag{4.11}$$

The term "stored power" refers to power stored in the form of heat within materials:[34][32]

$$P_{stored} = c \times M \times \frac{d}{dt}\Delta T \tag{4.12}$$

Where:

$C -$ *represents a measurement of a material's storage capacity*

$M -$ *represent the material's mass*

$\Delta T -$ *is the rate of increase in temperature per unit of time*

Dissipated power into the surroundings can be calculated by the [34][32]

$$P_{dissipated} = P_{con} + P_{conv} + P_{rad} = h \times A_{surface} \times \Delta T \tag{4.13}$$

Where:

$h -$ *represents the heat transfer co efficient*

$A_{surface} -$ *represens the heat emiting surface*

According to the Power Balance law:

$$P_{in} = P_{stored} + P_{dissipated} \tag{4.14}$$

As for the thermal time constant so by using the equations (4.11), (4.12) &(4.13) in equation (4.14).[32]

$$\Delta T(t) = \Delta T_e \left(1 - e^{\frac{t}{\tau}}\right) \tag{4.15}$$

$$\tau = \frac{cM}{hA_{surface}} \tag{4.16}$$

τ shows the time constant which is defined as the time required to reach the 63.2% from ΔT_e and t in time minute. The incremental change of the temperature in the system can be represented by the step functions with the ΔT_ecoefficient shows the maximum incremental when steady state. [35]

Overloading of the equipment is dependent on the thermal time constant. It means that if the thermal time constant is higher then the overloading time will be higher. It depends on the material properties as well as the mass of the object. For example, if the transformer has more mass that transformer can overload for more time e.g., for a few hours. But cables have low mass so the cable cannot overload like a transformer. It means that time constant is directly proportional to the mass if the cross-section of the cables is increased, their time constant is also increased. To find the time constant from the temperature graph let us take an example for better understanding. Figure 4.8 shows the temperature rise graph of another random device. The time constant of the upper curve can be found as.

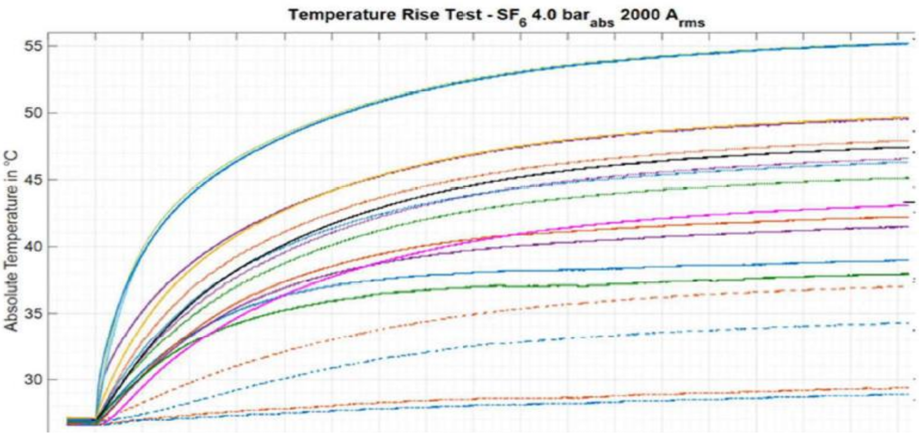

Figure 4-8:Temperature graph of random device[35]

The time required to attain a temperature change of 63.2 percent is known as the thermal time constant.

First, the temperature difference needs to find because the graph is not started from zero. So, the temperature difference is

$$\Delta T = 55℃ - 27℃ \tag{4.17}$$

$$\Delta T = 28℃ \tag{4.18}$$

$$63\% \text{ of the } 28℃=0.63 \times 28℃ \tag{4.19}$$

$$=17.64 \tag{4.20}$$

For this case

$$17.64+27=45℃ \tag{4.20}$$

So, from the graph, it is observed that the time required to reach this point is 1 Hour.

4.5.1 Thermal Conduction

Conduction heat is transferred from one molecule to nearby molecules when electrons collide in conducting materials like metals. Conduction heat is explained by the Fourier law in equation 4.21 which includes the special property called thermal conductivity. The thermal conductivity shows how easily material transfers heat. The thermal conductivity is depending on the nature of the material like thermal conductivity is highest for the metal. Whereas thermal conductivity is lowest for the gases. Any material which has a low thermal conductivity is considered a thermal insulator. [36]

$$P_{cond} = \lambda A_{cs} \nabla T \tag{4.21}$$

For simple applications, heat conduction is considered as one dimension so Fourier law is reduced to [36]

$$P_{cond} = \frac{\lambda}{s} A_{cs} \Delta T \tag{4.22}$$

Where :

$\lambda -$ thermal conductivity of the materials

A_{cs} $-$cross-sectional area

∇T $-$temperature gradient

s $-$distance over the temperature difference ΔT

Reciprocal thermal conductivity is thermal resistivity which is defined as the material's capability to resist heat flow. Different thermal resistivity, Conductivity, and specific heat capacity are explained in the tables 4.2.

Table 4-2:Thermal conductivity for different materials[37].[38].[39].[40]

Material	**Thermal conductivity $\boldsymbol{\lambda}$ [W/mK]**	**Thermal resistivity $\boldsymbol{R}\lambda$ [mK/W]**	**Specific heat capacity $\hat{c}$ [J/kgK]**
Aluminum	240	0.0042	900
Copper	385	0.0026	390
Steel	12-16	0.083-0.0625	490

4.5.2 Thermal Convection

Convection is the movement of fluids that circulates heat exchange between fluids and solid surfaces. Depending on how the fluid motion is carried out, convection is described as either forced or free. Newton's Law of Cooling, which has the heat transfer coefficient, is used to calculate convection. The heat transfer coefficient, like thermal conductivity, is a function of the fluid's thermophysical properties; however, it is also a function of the system's physical features, such as fluid velocity and flow field shape. The power is generated from the convection using Newton's law of cooling.[36]

$$P_{conv} = h_{conv} A_{surf} (T_s - T_o) \tag{4.23}$$

Where:

h_{conv} $-$heat transfer coefficient

A_{surf} $- s$urface Area

T_s $- s$urrunding Temperature

T_o $-$Ambient Temperature

Heat transfer coefficiency depends on the type, physical properties of the fluid, and the physical situation. Single-phase fluids (such as gases or liquids) or fluids that undergo a phase shift can be used to transfer heat via convection. Due to the extra energy necessary to evaporate or condense a fluid, such as through the latent heat of vaporization, solidification, sublimation, or crystallization, phase shifts can drastically increase heat transfer.[32]

4.5.3 Thermal Radiation

Thermal radiation is defined as the thermal motion of particles in a substance caused by electromagnetic waves even if there is no matter between them. All materials radiate radiation in all directions, regardless of temperature. Radiation energy transfer is unique in that it requires no conducting medium, unlike conduction and convection.[36]

Thermal radiation is emitted by an object which has an absolute temperature greater than zero and all materials around the object absorb the radiation. The intensity of the energy can be determined by the temperature of the surrounding objects and the temperature of the surface.

The power produced by the radiation is explained by the equation 4.24[36]

$$P_{rad} = \varepsilon \sigma_s A_{surf} (T^4 - T_0^4) \tag{4.24}$$

Where:

ε −emissivity of the surface 0≤ $\varepsilon \leq 1$

σ_s −Stefan Boltsmann constant

A_{surf} −radiating area

T −absolute temperature

T_0 −Absolute temperature of ambient walls

4.5.4 Current Carrying Capacity

The current capacity of the cable is defined as the maximum current that a cable can continuously carry without exceeding the temperature limits of the cable. The current rating is determined by how heat is dispersed through the cable surface and onto the surrounding environment. The current-carrying capability of a cable is determined by its temperature rating. The insulating material is largely responsible for the cable's maximum temperature rating. The generated heat in the cable is equal to the heat dissipated from the cable surface in a steady state. That is, the maximum steady-state temperature is determined by the cable components' thermal resistance as well as the ambient temperatures. The 25℃ or 30℃ consider the surrounding temperature for the cables in the air.[41]

Other factors are also important for the cable rating like conductor losses, sheath, armor losses, and internal and external thermal resistance. Metallic sheath losses are very important for the single-core conductor cables bonded and earthed at both ends.

There is logarithmic scale relation between temperature rise and time. Because it takes time to reach a steady-state, it can only carry more than the maximum continuous rating for a limited or short time. The overload factor is determined by the amount of initial loading. Because the short-circuit current can be 20 times or more than the loading current, the thermal and electromagnetic impacts are proportional to the square of the current.[41]

The European standard coordination specifications HD22.4 and HD22.12 are typically followed for producing and manufacturing electric car charging cable items in Europe. Ethylene-propylene rubber insulated, and ethylene-propylene rubber/chloroprene rubber are both specified by HD22.4. Table 4.3 shows the temperature limits of the polymeric cables.

Table 4-3:Conductor temperature limits of polymetric cables[42]

Insulating Compound	Continuous Temp [℃]	Short circuit Temp [℃]
Polyvinyl chloride (PVC)	70	160
Polyethylene (PE)	70	130
Ethylene propylene rubber (EPR)	90	250
Cross-linked polyethylene (XLPE)	90	250

4.6 IEC Limits

The IEC 62196-3 international standard specifies the requirements and tests for plugs, socket outlets, vehicle connections, and vehicle inlets used in electric vehicle conductive charging.Part 3 specifies that DC and AC/DC pin and contact tube vehicle couplings must be dimensionally compatible and interchangeable. According to the IEC 62196-3, there are ambient temperature limits for the contact, inlet port, and connector part. The maximum permissible temperature at the power contact is +80℃. When the temperatures reach this point the supply current will be reduced. It is also mentioned in the IEC 62196-3 that If the temperature touches the +90℃ then shut off the power supply. The charging process shut off if the temperature crosses this limit. So in this thesis +80℃ is considered the limit and compared the result with +80 ℃. But important thing is that these temperature limits change with the ambient temperature. Table 5-1 explains the ambient temperature limits during the operations.

Table 5-1: IEC Temperature limit of the Cable[46]

Terminal	Temperature limits
Contact	+80
Inlet part	-30℃ ...... +80℃
Connector part	-30℃ ...... +80℃

5 Thermal Modeling

Vehicle electrification helps to cut vehicle fossil fuel usage. This is one of the methods to meet the target of reducing greenhouse gas emissions. Fast charging using dc and a future charging power of 350 kW, which is designated as high-power dc charging, enable the charging of electric vehicles. The peak load for the entire charging path from the charging station to the car battery is 350 kW of charging power at currents up to 500 A. When such a high current passes through the cables, the electrical resistance of the cables generates heat loss. To avoid the overloading and overheating or the heating limits to remain within desirable values this heat loss must be incorporated into the design and dimensioning of all electrically conducting components. This heat loss can be accomplished by thermal management, which can estimate the exact status of all components in every portion of the system at any given time.[43]

The temperature of every component of the EV rises significantly when the DC power cable has a high current. This temperature rises more fastly when the vehicle is not moving because there is no convection available for the cooling. Therefore a complete thermal model is needed for the high power DC cable that helps to protect the system from overloading.

The major problem is the high current that passes through the cable and produced heating in the DC cable. This problem can be overcome by increasing the cross-section area of the cable and transferring the power at the same level of voltage. But in this way the weight of the cable is increased, the cost of the cable is also increased, and needs more space. For example, 50mm^2 and 95mm^2 cross-section areas of the conductor make a remarkable difference in terms of cost and weight. Another good option is that increase the voltage and transfer the power at a lower level of current but this option will also increase the weight of the cable. So changing the dimensions of the cable is not a good and feasible option to avoid overloading.[43]

5.1 Thermal Electrical Analogy

The thermal electrical analogy is used to explain the similarity between the diffusion of heat and electrical charge. Total heat loss is defined as the difference between the environment temperature and conductor temperature. Voltage is equivalent to temperature, current via an electrical circuit is equivalent to heat flow rate, and electrical resistance is equivalent to thermal resistance.

Table 5-1The units for thermal-electrical analogy[43].[32]

Electrical	Thermal
Charge	Heat
Current	Heat flow rate
Voltage	Temperature
Resistance	Thermal Resistance
Capacitance	Thermal Capacitance

Due to temperature differences, heat is transferred when voltage sends a current through the resistor. The physical form of transfer such as conduction, convection, and radiation is represented by the resistor. The stored equations of each component help to calculate the heat produced. This heat is depending on the applied current, voltage as well as ambient temperature. Using the electrical analogy concepts an equivalent circuit is explained in the figure. In the diagram heat dissipation is represented by the resistor and thermal capacities depend on the heat generation. Diagram 5.1 explains the transfer of heat in space by conduction and within the material by convection and radiation. Using the various techniques it is possible to model the individual components such as contact of the cable or the whole cable including the connector and inlet.

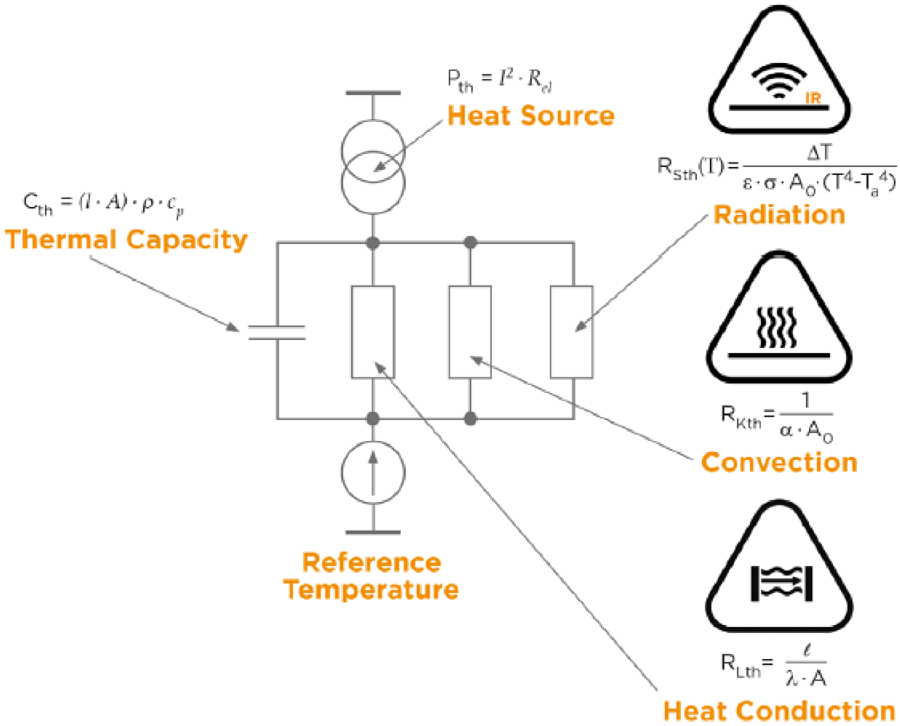

Figure 5-1:equivalent circuit diagram for thermal modeling, resistors represent the three ways of heat dissipation[43].

The thermal modeling of the charging cable is part of the thesis including the simulation. But due to the lack of time a general thermal model of the cable is explained with various techniques. Using the loop formation technique a thermal model of the charging cable is explained in figure 5.2 by using the above electrical analogy. This thermal model is help to find the temperature source, heat sinks, and when the temperature reaches the critical point. It also helps to find the adiabatic state and what is the impact of this state.

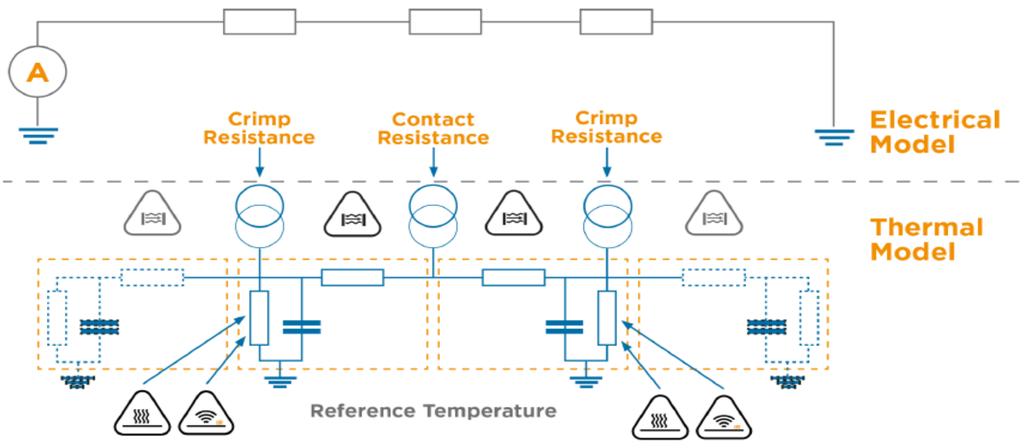

Figure 5-2:Electrical and thermal model of the cable[43]

6 Experimental Setup

In this chapter physical setup of the CCS-2 cable is explained and all other devices are used in the lab to measure the respective tests. The main setup is built in the High current lab at the University of South-Eastern Norway. The Skagerak Energi provides the Combined Charging System (CCS) type 2 cables. The setup is helped to analyze the thermal properties of the CCS-2 charging cable. The supplementary equipment is provided by the USN to perform the desired tests. A total of eighteen thermocouples are mounted on the cable for temperature and resistance measurement.

6.1 Supplementary Equipment

6.1.1 Thermocouples

Temperature sensor with Chromel and Alumel conductors that meets the output standards specified in ANSI/ASTM E230 or IEC 60584. Thermocouples type K is used to measure the voltage, Temperature across the cables. Type K is very common due to accuracy and reliability. It has a wide temperature range to measure. The temperature range of Type K thermocouples is -200 to 1260°C.

6.1.2 Data Logger & Connection Box

Keysight 34972A is a Data Logger that is used to capture data over time for a range of applications. A data logger collects and documents data on a 24-hour basis using internal memory and sensors. Keysight 34972A is used to collect temperature values across the cable. Figures 6-2 show the Keysight 34972 A data logger. A connection box is used to connect the thermocouples with a data logger for scanning. A connection box is shown in figure 6-1.

Figure 6-1:Connection box

Figure 6-2:Data logger

6.1.3 Current Injection tester

A current injection tester is used as the power supply. A test current is injected into the primary side of the system and sees the effect on the system. Figures 6-3 show the current injection tester which is used in the lab.

Figure 6-3:Current injection tester[44]

6.1.4 DC supply

SM 15-100 DC Power supply is used to supply 50A DC for the DC resistance test measurement. Figures 6-4 show the SM 15-100 DC supply.

Figure 6-4:DC supply

6.1.5 Others Equipment

- METRA HIT 30M voltmeter is used to measure the voltage across the cables at a different point.
- Measurement Rules Are used to measure the length of the connector and inlet part of the cables as well as also for the contact length measurement.
- A wire stripping is used to remove the insulation of the wires for good connections.
- A cordless drill is used to make the holes in the cable for the thermocouple’s connection.

6.2 Sensor Setup

The total length of the CCS-2 is 1214 cm including the contact length. The cable is divided into three parts for the measurement. One is the inlet part, the second is a connector and the third one is the contact of the cable. Only the DC part of the CCS-2 cable is selected for the thermal observation which is DC+ and DC- The inlet part has the same color for both phases whereas the connector part has one black which represents the DC- and the other one red which represents the DC+. A total of eighteen thermocouples are mounted on the whole cable.

6.2.1 Inlet part

The total length of the inlet part is 200 cm. So three points are selected to get more data about the thermal characteristics of the inlet part. The cable shoe is connected at the start point of the inlet part which helps to make a good connection with the power supply. Figure 6.4 shows the position of the sensor measuring points. Table 6.1 shows the distance between the thermocouples from one to another.

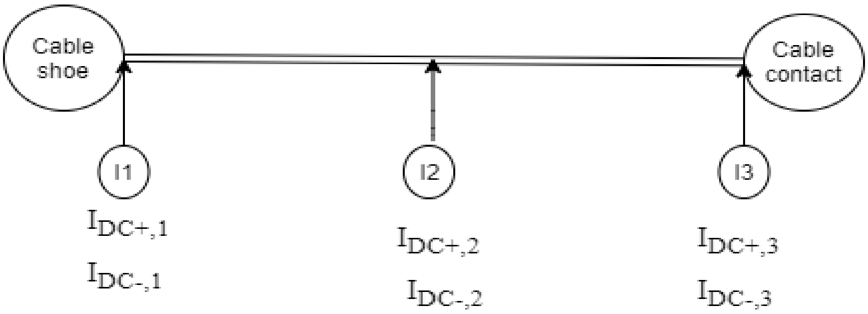

Figure 6-4:Thermocouples position at Inlet part

Figure 6.5 shows the method of mounting thermocouples on the inlet part. The thermocouples are mounted on the conductor by drilling a hole through the cable insulation to the conductor surfaces. As mentioned above two cables are selected so a total of six thermocouples are installed at different three measuring points. Figure 6.4 I1 represents the two thermocouples one for DC+ and the other for DC-.Same for I2 and I3 denoting the two thermocouples respectively.

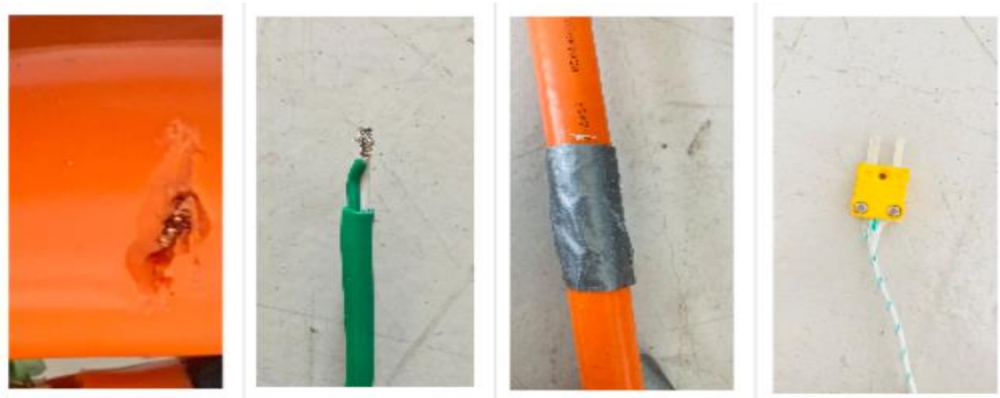

Figure 6-5:Method of thermocouples installation

Table 6-1:Distance between thermocouples at Inlet part

Start Point	End Point	Distance[cm]
I1	I2	112
I2	I3	88
I1	I3	200

6.2.2 Connector Part

The total length of the connector part is 990 cm. Five different points are selected on each cable for the measurement. The end of the connector is shorted to make the star load. Figure 6.6 shows the position of the thermocouples and table 6.2 the distance between them.

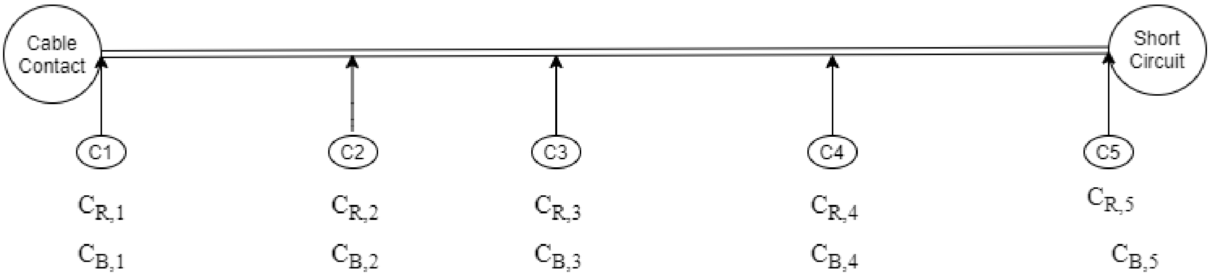

Figure 6-6:Thermocouples position at connector part

The same procedure is applied for mounting the thermocouples on the connector part as shown in figure 6.7. A total of ten thermocouples are installed on the connector part. Each point represents two thermocouples one for red and one for black cable.

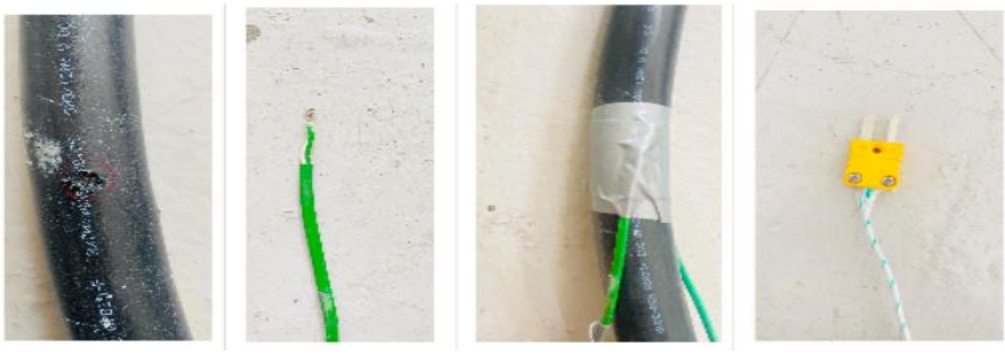

Figure 6-7:Method of thermocouples installation at connector part

Table 6-2:Distance between thermocouples at connector part

Start point	Endpoint	Distance[cm]

C1	C2	291
C2	C3	227
C3	C4	252
C4	C5	220
C1	C5	990

6.2.3 Cable Contact

The cable contact is the most important for the thermal characteristics of the CCS-2 cable. So thermocouples are placed inside the contact. There is no other option available to measure the temperature of the contact. So thermocouples wires are placed inside the connector port and then the inlet part is connected to the connector by applying a small force as shown in figure 6.9. There is a possibility of error because the thermocouples start to measure the temperature when two wires are connected. So it is not 100% sure that these wires are connected at the end of connector contact. The thermocouples wire in the connector is shown in figure 6.8.

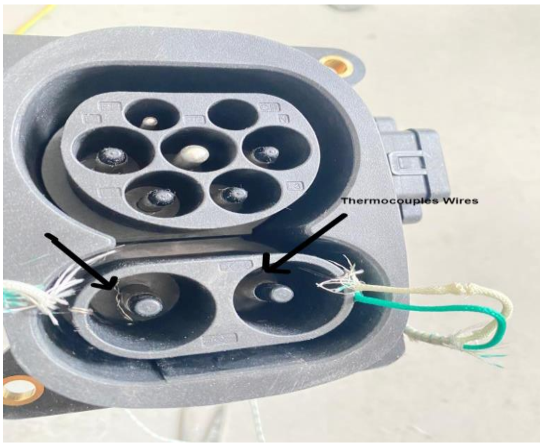

Figure 6-8:Thermocouples wires for the Contact

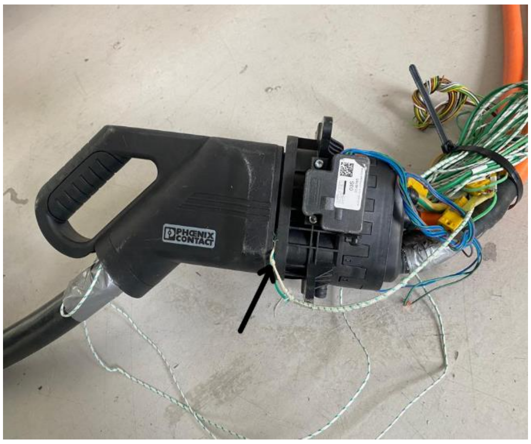

Figure 6-9:Cable contact

6.3 Thermocouples Descriptions

For a better understanding of figure 6.4 and figure 6.6, the thermocouples description with a port number from the connection box is explained in table 6.1

Table 6-3:Thermocouples Position

Port Number	Label	Descriptions
101	$I_{DC+,1}$	DC+ cable of the inlet connected with power supply

102	$I_{DC-,1}$	DC- a cable of the inlet connected with the power supply
103	$I_{DC+,2}$	DC+ cable of the inlet part
104	$I_{DC-,2}$	DC- a cable of the inlet part
107	$I_{DC+,3}$	DC+ cable of the inlet near to the contact
108	$I_{DC-,3}$	DC- cable of the inlet
112	Contact_1	Cable contact
113	Contact_2	Cable Contact
302	$C_{R,1}$	Red cable of the connector part near the Contact
303	$C_{B,1}$	Black cable of the connector part near the Contact
305	$C_{R,2}$	Red cable of the connector
306	$C_{B,2}$	Black cable of the connector
308	$C_{R,3}$	Red cable of the connector
310	$C_{B,3}$	Black cable of the connector
311	$C_{R,4}$	Red cable of the connector
314	$C_{B,4}$	Black cable of the connector
315	$C_{R,5}$	Red cable of the connector
316	$C_{B,5}$	Black Cable of the connector

6.4 Test Object

The test object is the Combined Charging System (CCS-2) cable connected to the power supply.CCS-2 cable can be used for both AC and DC charging at the charging station. The inlet

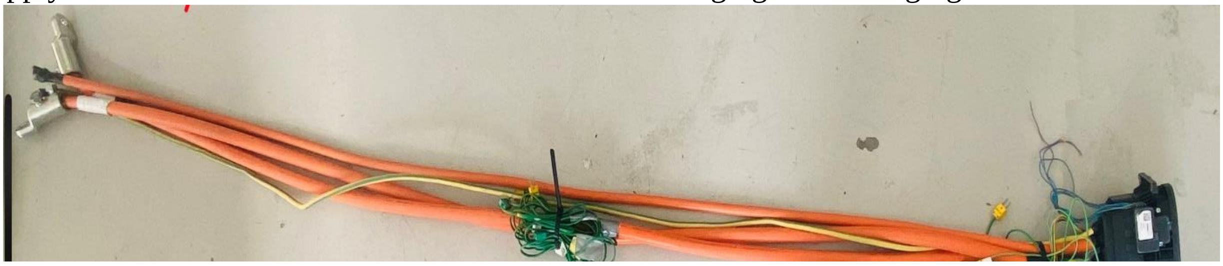

Figure 6-10:Cable inlet part

part has three phases of AC charging along with the two ports of DC at the bottom of AC pins. The proximity and control pilot pins are used for the communication between the inlet and connector parts. The inlet part cable is designed and used according to the standard IEC 62196-3. In this thesis, only the DC part of the inlet cable is considered.AC cables with protective earth pins are covered with insulation for protection during the experiments. It can provide 250 A continuous charging. The Inlet part of the cable is shown in figure 6.10.

The connector part of the CCS-2 charging cable is used exclusively for DC charging. The connector part has two DC ports with some additional ports for communication. The connector part is designed and used according to the IEC-62196-3 standard.The connector is shown in the figure 6.11

Figure 6-11:Connector part

Figures 6-12 show the CCS-2 inlet part on the right side and the connector part on the left side with pins descriptions.

Figure 6-12: CCS2 inlet and connector with pin descriptions[45]

The technical specification such as rated voltage, rated current, cable structure, and temperature limits of the inlet part is explained in table 6.2. But the important point is that this temperature limit is the ambient temperature. Every place has a different temperature so temperature limits are changed accordingly. According to the IEC 62196-3, the extreme temperature limit of the inlet part is +90℃ if the temperature reaches this limit then the power supply shut off. In the specification, it is also mentioned that if the temperature reaches +80℃ then decrease the supply current. So in this thesis +80℃ is considered the limit and perform the experiments accordingly.

Table 6-4:Technical data of inlet part[46]

Technical Data	3AC32DC250
Standard	IEC 62193-3
Rated DC current and Voltage	250A/1000V DC
Rated AC current and voltage	32A/480V AC
Cable structure AC Sheathed cable(Shielded)	4 x 6.0mm^2
Cable structure signal contact(single core wire)	7 x 0.5mm^2
Insulation Resistance between contact	200MΩ
Ambient Temperature (during operation)	-40℃ .... +60℃
Ambient Temperature (storage)	-40℃ .... +85℃
Insertion Cycles	>10.000
Degree of protection(not plugged in)	IP67/IP55

The technical specification of the connector part such as rated voltage, current, and cable structure dimensions are mentioned in table 6.3 The temperature is the ambient temperature limit for the connector also. So as the ambient temperature is changed according to the place so temperature limits are changed according to the environment. According to the IEC 62196-3, the temperature limit for this part is also +90℃ but remember that this is the extreme limit. After reaching this point the power supply is shut down. So +80℃ is considered the limit in this thesis and perform experiments according to the limit.

Table 6-5:Technical data of connector[46]

Technical Data	3AC32DC250
Standard	IEC 62193-3
Charging Mode	Mode 4
Rated Current	250 A DC
Rated Voltage	1000V DC
Cable structure,Power Contacts	2 x 70mm^2 +1 x 35mm^2

Cable structure ,Signal contact	3 x 2 x 0.75 mm^2
Resistor Coding	1500Ω
Ambient Temperature (During operation)	-30℃ …. +50℃
Number of power contact	3(DC+,DC-,PE)
Surface Material of contacts	Ag
Insertion Cycles	>10.000
Degree of protection (unplugged)	IP20

6.4.1 Cable setup

Normally the connector part relates to the power supply and the inlet part is placed inside the vehicle. But here in the lab, the Inlet part is connected with the supply, and the connector part is shorted. The reason for this connection only passes the current through the cable for measurement. To make a good connection, a cable shoe is connected to the start point of the inlet part which is connected to the Power supply as shown in the figure. 6.14 The end of the connector is shorted to complete the circuit and make a star load as shown in figure 6.13

Figure 6-14:Cable shoe to connect with power supply

Figure 6-13:Short circuit at the end of connector

After mounting the thermocouples on the cable and other necessary connections. The inlet part is connected with the power supply which is DC supply in case of DC resistance and for the rest of the experiments AC injection transformer. Figure 6.15 shows the connection of the inlet with the power supply. Before the start of the experiment, thermocouples are tested using the connection box with the data logger, and the data logger uses the software Agilent BenchLink Data Logger 3 to collect data from the experiments to make sure the readings are understandable.

As CCS-2 cable is DC fast charging so DC supply should be applied for the measurement. But DC supply in the USN lab can provide only 100A DC so for the DC resistance test this power supply is used as the current need is 50A DC. But for the temperature and overloading tests, the rated current of the cable is 250A DC.So for the temperature rise and overloading tests the AC supply is used to supply 350A AC.So current injection transformer is used which can supply up to 2500A AC.

Figure 6-15:Inlet connection with power supply

The main cable setup is shown in figure 6.16. The blue one in the figure is the current injecter. Orange cables are the inlet part and black cables represent the connector part. S_1 and S_2 are the starting point of the setup. The E represents the endpoints of the cable and the endpoint is shorted with the help of a copper bar. There are eighteen thermocouples so two connection boxes are used which are connected through yellow wires with a data logger. The green wires are the thermocouples.

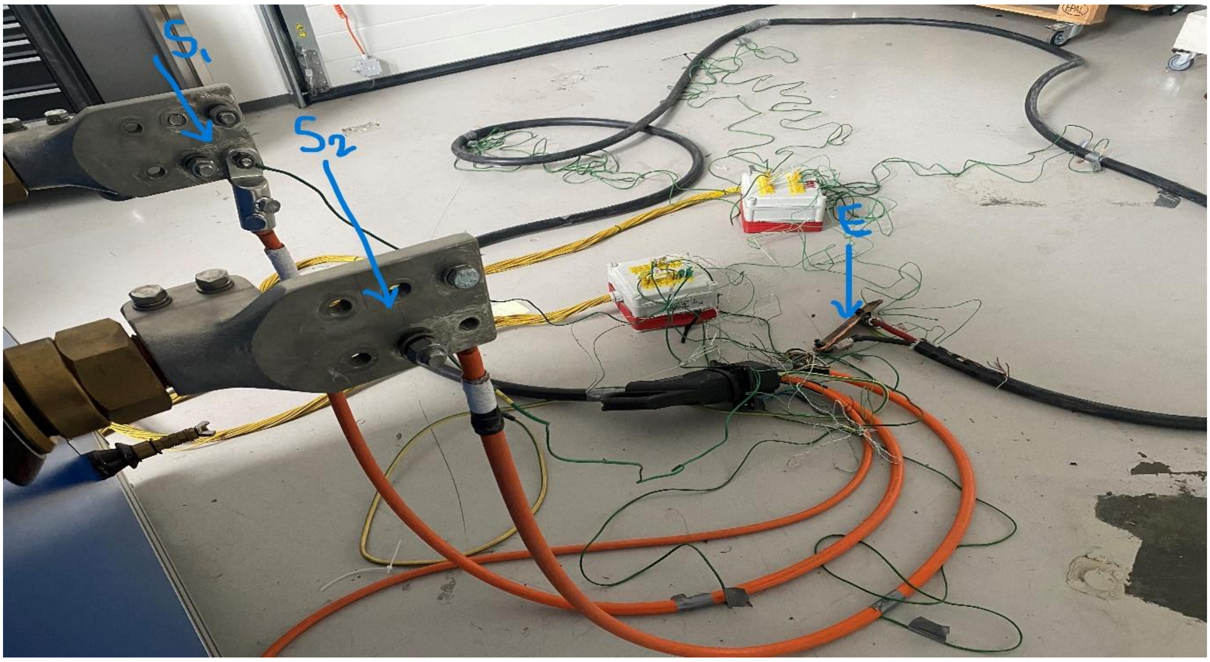

Figure 6-16:Cable setup

7 DC Resistance Test

7.1 Introduction

The resistance measurement of the CCS-2 EV cable is the first test for the Master thesis Subject 2022. The practical setup of the CCS-2 cable is made in the High Current lab at the USN Porsgrunn campus.

7.2 Purpose

In this test, the resistance of the CCS-2 EV cable is determined under no-load conditions (at Room Temperature). This is an important and the first step to finding the thermal overloading of the CCS-2 cable at normal operations. The purpose of this measurement is to determine the:

- Per unit length resistance of the cable
- The Bulk resistance of the two cables.
- The contact resistance of the cables.
- The total resistance of the cable

7.3 System Descriptions and Measuring Techniques

The cable setup with the thermocouples between them is explained in Figures 6.4 & 6.6.

Three parts are considered for the resistance measurement i.e., the Contact of the cable, the Inlet part, and the Connector part.

Procedure:

- Apply 50A DC and measure the voltage drops across the contacts of the cables by using the thermocouples points. The reason behind applying 50A DC is to avoid the cable from heating. Because if the temperature of the cables is increased then resistance is also increased. So the actual resistance of the conductor cannot measure when the cable is getting heat.
- With the help of thermocouples, the voltage drops across a specific length of the inlet are measured while applying the 50A DC.
- The same procedure is done for the resistance of the connector part.

7.4 Performance of the Experiment & results:

This part explains the test and the results are calculated. The results are presented in a table.

7.4.1 Bulk Resistance Measurement of the inlet

The bulk resistance of the inlet part is calculated by applying the 50A DC and measuring voltage drops across the inlet part. From figure 6.4 the voltmeter probes place at I1 and I3 and measure the voltage across them. By using the equations 4.6 and 4.7.

$$\boldsymbol{R_{Inlet}} = 373\boldsymbol{\mu\Omega} \tag{7.1}$$

7.4.1.1 Measured Resistivity of the inlet port

In this section, the resistivity of the materials is calculated from the measured resistance. The length of the inlet part is shown in Figure 6.4 and the area of cross-sections is explained in table 6.2. From equation (4.3)

$$\boldsymbol{\rho_{inlet}} = 1.77\ \boldsymbol{X}\ 10^{-8}\ \boldsymbol{\Omega} \qquad \boldsymbol{m} \tag{7.2}$$

7.4.1.2 Theoretical Estimations of the Inlet Bulk Resistance

The cross-sectional area, length, and resistivity of the material are known. So Theoretical resistance can be found using equation (4.3). The material of the cable is copper so the resistivity of copper is:

$$\rho = 1.68\ X\ 10^{-8}\Omega m \tag{7.3}$$

$$\boldsymbol{R_{inlet}} = 354\ \boldsymbol{\mu\Omega} \tag{7.4}$$

7.4.1.3 Inlet Resistance Measurement with Different Length

In this section find the resistance of a specific length and then calculate resistance per unit length. After that resistance per unit, length is compared with the resistance per unit length which is calculated from the bulk resistance of the inlet part in table 7-1. By using figure 6.4 the probes of the voltmeter are placed at I1 and I2.So by using the equations 4.6 and 4.7.

$$\boldsymbol{Resistance\ per\ cm} = 1.82\ \boldsymbol{\mu\Omega}/\mathbf{cm} \tag{7.5}$$

7.4.1.4 Conclusion:

In conclusion, Table 7-1 compare all values of resistance-related inlet part. . From table 7-1 it can be seen the measured resistivity of the inlet is 177 $\mu\Omega m$ whereas the expected resistivity of the inlet cable is 168 $\mu\Omega m$. There is a small difference between the expected and measured values. It may be due to different alloy resistivity. The resistance per unit length from different lengths is 1.82 whereas the resistance per unit length from the bulk resistance is 1.87. There is a small difference between the values which is possible due to the systematic error, not exact distance during calculations, and personal error. But the difference is not too much which can be ignored.

Table 7-1:Inlet Resistance Measurement

Start	End	L(start-end) [cm]	V[mV]	R [$\mu\Omega$]	$R/_{L}$ [cm]	$\rho[\mu\Omega m]$
I1	I2	88	8.02	160	1.82	
I1	I3	200	18.67	373	1.87	177
Average:					1.84	

7.5 Bulk Resistance Measurement of the Connector part

In this section, the bulk resistance of the connector is calculated. Apply the 50 A DC and place the voltmeter probes at C1 and C5 according to figure 6.6. So by using the equations 4.6 and 4.7.

$$\boldsymbol{R_{connector}} = 2520\boldsymbol{\mu\Omega} \quad (7.6)$$

7.5.1 Measured Resistivity of the connector part

In this section, the resistivity of the connector part is calculated by the calculated resistance from equation 5.2. Figure 7-1 is used to find the length of the connector part. The cross-section area of the connector is explained in table 6.3. The material of the cable is copper and resistivity is explained in 4.1

$$\boldsymbol{\rho_{connector}} = 1.78\ \boldsymbol{X}\ 10^{-8}\ \boldsymbol{\Omega} \qquad \boldsymbol{m} \quad (6.7)$$

7.5.2 Theoretical Estimations of the connector Bulk Resistance

The main reason to find the theoretical estimation is to compare the values with calculated values in section 7.5. The length of the connector can be estimated in figure 6.6. The cross-area of the connector is mentioned in table 6-3.

$$\boldsymbol{R_{connector}} = 2376\ \boldsymbol{\mu\Omega} \quad (6.8)$$

7.5.3 Connector Resistance Measurement with Different Length

In this section, the resistance per unit length from a specific length is measured instead of the bulk resistance measurement. The resistance per unit length is compared with the above resistance per unit length from the bulk resistance measurement as mentioned in table 7-2. Figure 10 shows the specific length and Voltmeter probes. The Voltmeter probes are placed at the C4 and C5 according to figure 6.6.By using the equations 4.6 and 4.7.

$$\boldsymbol{Resistance\ per\ cm} = 2.5\ \boldsymbol{\mu\Omega}/\mathbf{cm} \tag{6.9}$$

7.5.4 Conclusion

In short, Tables 7-2 compare the expected and measured resistance of the connector. The resistivity of the pure copper is 168 $\mu\Omega m$ whereas the resistivity from the measured values is 178. As seen there is a difference between the expected and measured. One of the possible reasons due to the resistivity of the material alloy.

Table 7-2:Connector resistance measurement

Start	End	L(start-end) [cm]	V[mV]	R [$\mu\Omega$]	$R/_L\ \mu\Omega\ [cm]$	$\rho[\mu\Omega m]$
C3	C4	220	28.04	561	2.55	
C1	C4	990	126	2520	2.54	178
Average:					2.54	

7.6 Contact Resistance of the Cable

In this section, the contact resistance of the cable is determined. The contact resistance is very important because CCS-2 is DC fast charger. So Characteristics of contact are very important. Contact of the cable is the main part to check the thermal overloading of the charging system. Figure 7-1 shows the point of the voltmeter while applying the 50A DC. The point that needs to remember is that while measuring the voltage drops placed the probes as close to contact in order to avoid the bulk resistance in contact resistance.

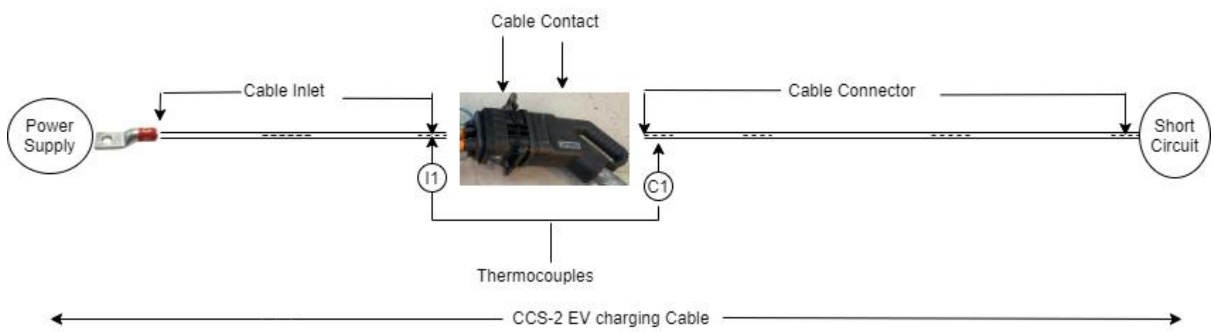

Figure 7-1:Cable contact resistance measurement

By using equations 4.6 & 4.7:

$$\boldsymbol{R_{contact}} = 146.6\boldsymbol{\mu\Omega} \tag{6.10}$$

7.6.1 Contact Resistance from the Bulk Resistance of the inlet & Connector

In this section, contact resistance is calculated from the resistance of the inlet, and connector and then compare with values that are calculated from direct contact measurement. Figure 7-2 explains the measuring voltage probes. First, find the R_tot from the voltage drops. As the length of the inlet and connector part can be seen in Figures 6.4 & 6.6. Resistance per unit length of the inlet and connector is known so by using the resistance per length to find the resistance of R1 and R2 parts respectively. In the end, the resistance of parts is subtracted from the R_Tot to find the contact resistance.

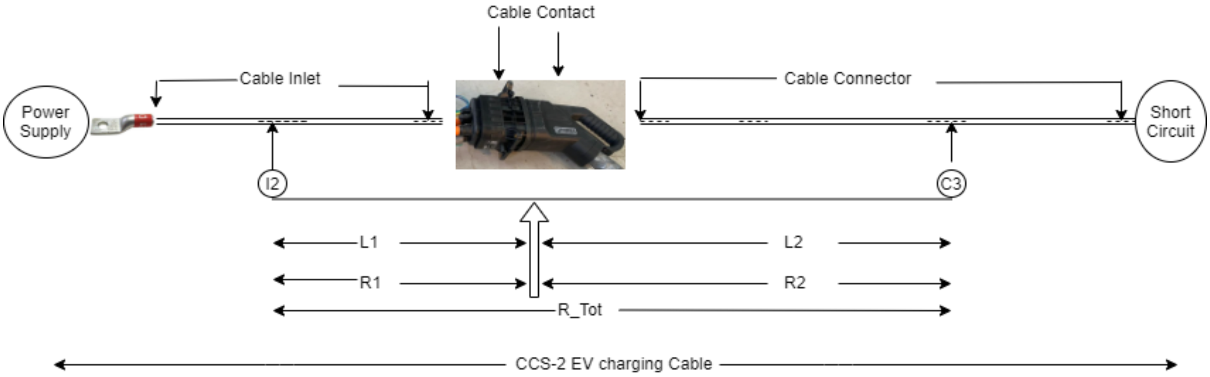

Figure 7-2:Contact resistance measurement from bulk resistance

By using equations 4.6 & 4.7.

$$\boldsymbol{R_{Tot}} = 2260\boldsymbol{\mu\Omega} \tag{6.11}$$

$$\boldsymbol{Resistance\ of\ inlet\ part} = \boldsymbol{R}1 = 183\ \boldsymbol{\mu\Omega} \tag{6.12}$$

$$\boldsymbol{Resistance\ of\ connector\ part} = \boldsymbol{R}2 = 1991\ \boldsymbol{\mu\Omega} \tag{6.13}$$

$$\textbf{Contact}\ \boldsymbol{Resistance}\ = \boldsymbol{Rtot} - (\mathbf{R1} + \mathbf{R2}) = \mathbf{84}\boldsymbol{\mu}\mathbf{\Omega} \tag{6.14}$$

Table 7-3:Contact resistance measurement

Contact Resistance:	
$\text{Resistance}_{\text{Direct}}$	$146.6\mu\Omega$
$\text{Resistance}_{\text{Total}}$	$84\mu\Omega$

7.7 Discussion

The results in tables 7-1,7-2 and 7-3 show the comparison between all parameters. There is a small difference between them. Possible reasons are:

Different resistivity of the materials. The material of the contact is silver coated and the material of the cable is copper so this is the reason for the difference in contact resistance.

The second reason for the difference in contact reason is the addition of bulk resistance with contact resistance. There is only one option to measure the voltage drop across the cable contact and that is to make a hole near the contact and place a measuring probe inside the hole for voltage drops. The hole is made as close to the contact as possible. But some bulk resistance is included in the measurement which is explained in section 7.6. So section 7.6.1 explains how the bulk resistance is excluded from the contact resistance. In section 7.6 calculation, the small resistance of the inlet and connector is included in the contact resistance. In order to remove the small resistance of the inlet and connector from the contact resistance, a resistance per unit length of the inlet and connector is calculated.R1 is calculated with the help of resistance per unit length and length of the inlet part until contact. The same calculation is done for the R2 Add the value of R1 and R2 and then subtract the value from R_{tot} in sections 7.6.1. In this way, bulk resistance is removed from the contact resistance.

The third reason is the resistance of the cable depends on the length and cross-section area. As length and area of each part are not exactly equal either. So, the resistance of each part will be different.

The fourth reason is that the distance between thermocouples and the total length of the cable is measured by the tape meter. So error can be possible in the length measurement which is also a cause of the difference.

Now there are many reasons to perform the DC resistance test.DC resistance of the cable depends on the dimensions, temperature, and resistivity of the materials.

The DC resistance test is very simple to perform but it is very important to check the quality of the cables. It can help to check the amount or quality of conductor material is enough or not.

The DC resistance measurement indicates how easily the current flow through the conductor. If the resistance of the cable is higher then a low current will flow through the conductor.

When the resistance of a conductor is high then more heat is generated from the conductor which can damage the insulation of the conductor.

All the above findings will help to make an idea about the cable conductor, heat loss, and increase of the temperature in the conductor.

Now power loss of the cables can be calculated while charging the battery for the emission-free construction. Resistance of the cables also helps to make a rough estimation of the rise of temperature during fast charging to charge the batteries for the construction site.

8 Temperature rise test with rated current

8.1 Introduction

This test is centered around the measuring of temperature rise of the Combined Charging System (CCS-2). When a rated current 250A DC is applied, the temperature will rise, and resistance will change as a result temperature will rise. The rated current is used until a stable temperature is attained.

8.2 Objectives

- Measuring the final temperature
- Compare the final temperature with the limit
- Calculate the time constant from the temperature rise.

8.3 Statement of Purpose:

This test will describe the effect the rated current has on the current path and the CCS-2 temperature rise. In the end, the temperature rise of the cable will compare with the limit provided by the IEC-62196-3 Temperature rise test.

8.4 System Descriptions and Measuring Techniques

The cable setup with the thermocouples positions is explained in figures 6.4 & 6.6. The cable description is explained in chapter 6 section 6.4

Three parts are considered for the temperature rise measurement. i.e., the Contact of the cable, the Inlet part, and the Connector part.

8.5 Results & Discussion

8.5.1 Temperature rise

The result of the temperature rise from the software as shown in table 8-1

Table 8-1:Temperature rise data

Port Number	Label	Descriptions	Initial Temperature[°C]	Steady-state Temperature[°C]	Temperature rise[°C]
101	$I_{DC+,1}$	DC+ cable of the inlet connected with power supply	20.97	28.59	7.62
102	$I_{DC-,1}$	DC- a cable of the inlet connected with power supply	21.23	26.84	5.61
103	$I_{DC+,2}$	DC+ cable of the inlet part	21.23	41.02	19.79
104	$I_{DC-,2}$	DC- cable of the inlet part	20.72	32.94	12.22
107	$I_{DC+,3}$	DC+ cable of the inlet near to the contact	22.80	67.07	44.27
108	$I_{DC-,3}$	DC- cable of the inlet	22.84	68.39	45.55
112	Contact_1	Cable contact	20.90	44.52	23.62
113	Contact_2	Cable Contact	21.54	39.48	17.94
302	$C_{R,1}$	A red cable of the connector part near the Contact	22.56	69.62	47.06

303	$C_{B,1}$	Black cable of the connector part near the Contact	21.12	63.12	42
305	$C_{R,2}$	Red cable of the connector	21.08	56.76	35.68
306	$C_{B,2}$	Black cable of the connector	21.16	58.72	37.56
308	$C_{R,3}$	Red cable of the connector	21.43	54.71	33.28
310	$C_{B,3}$	Black cable of the connector	22.18	63.32	42.93
311	$C_{R,4}$	Red cable of the connector	22.17	53.57	41.14
314	$C_{B,4}$	Black cable of the connector	21.56	52.40	30.84
315	$C_{R,5}$	Red cable of the connector	21.66	51.83	30.17
316	$C_{B,5}$	Black Cable of the connector	21.63	51.26	29.63

8.6 Thermal Time Constant

Now thermal time constant is calculated from the temperature rise graph. 18 thermocouples are installed at different positions as explained in Figures 6.4 & 6.6. The thermocouples are connected with a data logger which relates to the computer and by the software following graph is obtained.

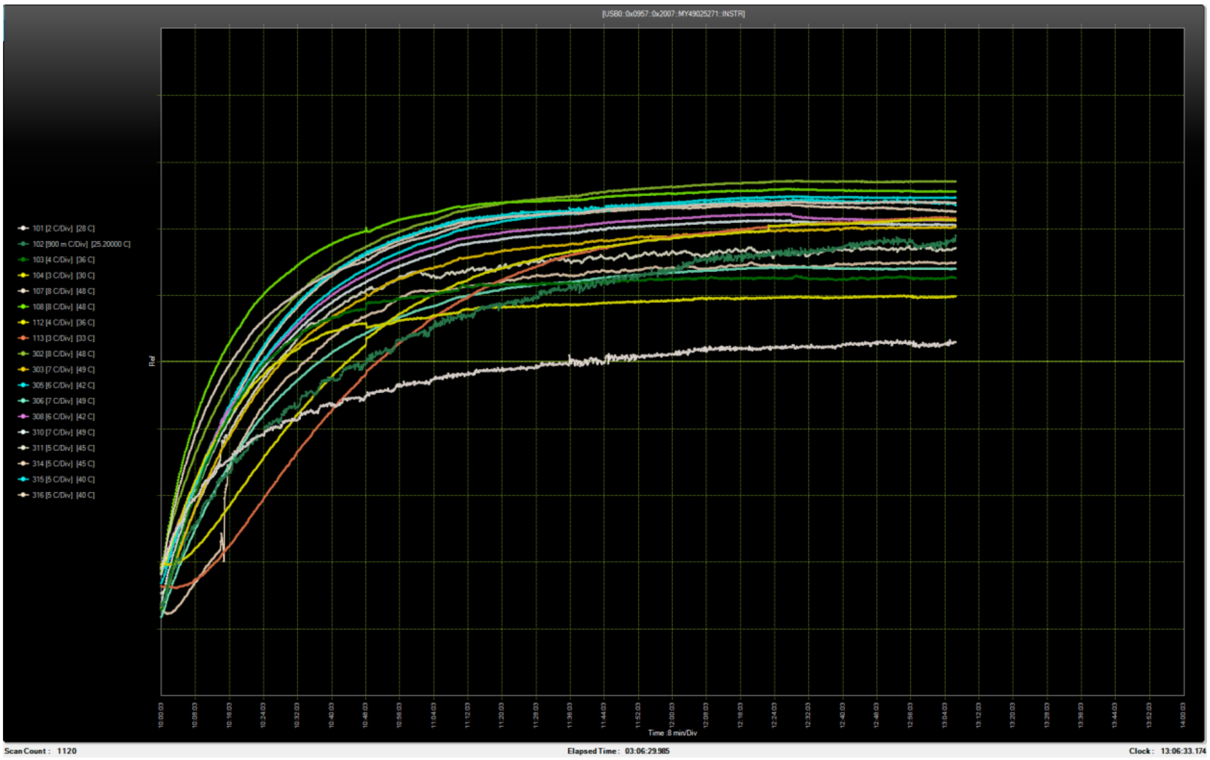

Figure 8-1:Temperature rise graph

Procedure to find the thermal constant is explained in chapter 4 and section 4.5. To get the thermal constant, Matlab is used for a clear picture of the graph. Data is imported into the Excel sheet file and using MATLAB get a clear graph of the temperature. Figure 8-2 shows the graph of temperature rise using MATLAB. Table 8-2 explains the thermal constant of the different parts of the cable. The thermal constant is represented in minutes.

Table 8-2:Thermal time constant

Port Number	Label	Descriptions	Initial Temperature[°C]	Steady-state Temperature[°C]	Thermal Constant[mins]
101	$I_{DC+,1}$	DC+ cable of the inlet connected with power supply	21.0	28.6	23.2
102	$I_{DC-,1}$	DC- a cable of the inlet connected with power supply	21.2	26.8	35.5
103	$I_{DC+,2}$	DC+ cable of the inlet part	21.2	41.0	18.2

104	$I_{DC-,2}$	DC- cable of the inlet part	20.7	32.9	19.7
107	$I_{DC+,3}$	DC+ cable of the inlet near to the contact	22.8	67.1	20.3
108	$I_{DC-,3}$	DC- cable of the inlet	22.8	68.4	17.7
112	Contact_1	Cable contact	20.9	44.5	42.9
113	Contact_2	Cable Contact	21.5	39.5	49.9
302	$C_{R,1}$	A red cable of the connector part near the Contact	22.6	69.6	25.2
303	$C_{B,1}$	Black cable of the connector part near the Contact	21.1	63.1	26.0
305	$C_{R,2}$	Red cable of the connector	21.1	56.8	27.0
306	$C_{B,2}$	Black cable of the connector	21.1	58.7	27.0
308	$C_{R,3}$	Red cable of the connector	21.4	54.7	25.7
310	$C_{B,3}$	Black cable of the connector	22.2	63.3	24.3
311	$C_{R,4}$	Red cable of the connector	22.17	53.6	20.67
314	$C_{B,4}$	Black cable of the connector	21.56	52.4	22.83

315	$C_{R,5}$	Red cable of the connector	21.66	51.8	23.17
316	$C_{B,5}$	Black Cable of the connector	21.63	51.3	23.5

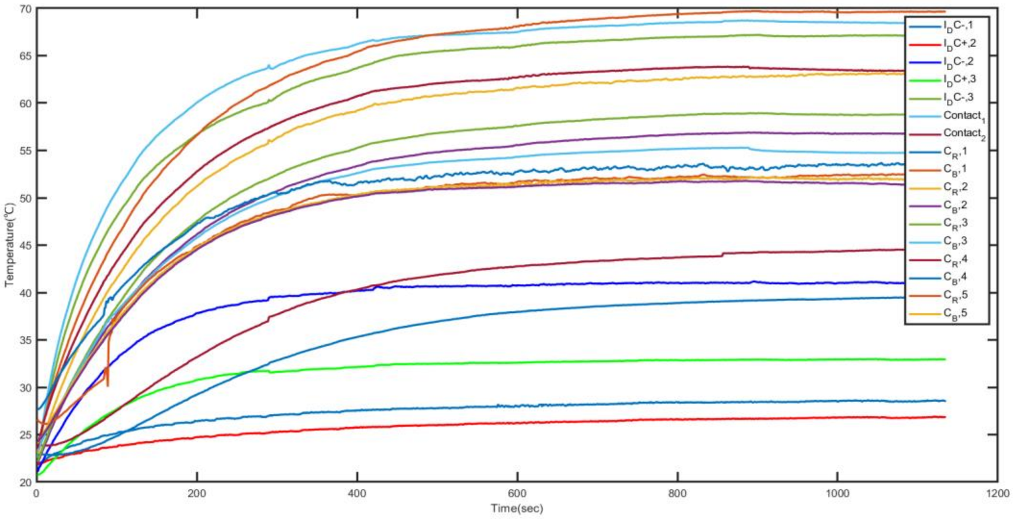

Figure 8-2:Temperature rise graph using Matlab

8.7 Discussion

From the tables 8-1, and 8-2. Contact temperature does not cross the limit and satisfies the steady-state condition of the IEC standard. There is a one or two points difference in the results. According to the energy balance, the temperature of the object is changed with time and the position of the measuring point. This could be the reason for the difference as there is a small gap between measuring points. Time constant has a close relation with heat transfer mode. As heat flowing is different along the cable so thermal time constant has some difference between the values. The inlet part which is connected to the power supply is opened that's why has the lowest temperature rise. The important thing to note is that contact temperature does not cross

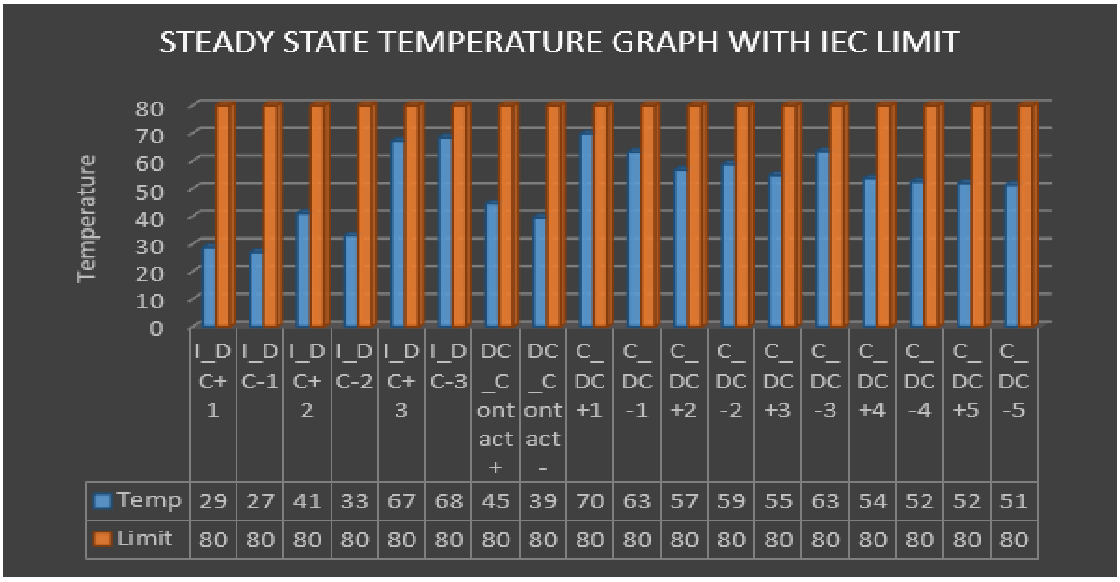

Figure 8-3:Steady state temperature with IEC limit

80 ℃ *and* temperature reaches a steady state. In the datasheet, it is mentioned that the +80℃ is acceptable but not more than +80℃. If the temperature increases the 90℃ then shut off the

power supply To avoid damage to the cable. So 80 ℃ is considered the limit for the temperature rise of the CCS-2 cable. Figure 8-3 shows the comparison of the steady-state temperature of the CCS-2 cable. The whole test takes approx. 3 hours to move to a steady-state.

From Figures 8-3. It is seen that the steady-state temperature of the contacts is low as compared to the temperature of the connector and inlet part near the contact. So, there is the possibility of an error during the measurement of the contact. Section 6.2.3 explains how the thermocouple wires are inserted into the DC contact for temperature measurement. As thermocouples measure the temperature where the wires first connect with other. So there is no possibility to measure the exact temperature of the DC contact with thermocouples. That's why it has an error in reading.

The inlet part which relates to the power supply has the lowest temperature because these are opened. Many factors affect the temperature rise performance of the cable. The first design of the cable such as the contact resistance of the cable, load current capacity, charging time, cable cross-sectional area, and selection of the materials.[47]

The heat generated by the current flow in the cable is transferred to the surrounding environment through the cable's metallic layer and insulation. Heat is energy that is transferred from one system to another when a temperature gradient exists. There are three heat transfer mechanisms conduction, convection, and radiation.

Due to the conduction phenomena, heat is transferred from the conductor surface of the cable to the insulation surface during this test. Then Convection and radiation phenomena occur from the cable surface to the surrounding environment. In this way, heat is flowing along the cable.

As this is fast charging cable cause of generating high heating. High heating puts a lot of stress on the cable parts. So high heating affects the parts of the cable and decreases the life of parts. If the temperature increases beyond the maximum limit then it has severe damage in the shape of fire. That’s why a temperature rise test is performed to check that the cable does not overheat during the charging of batteries in the emission-free construction site.

9 Temperature rise test with Overload current

9.1 Introduction

This test is centered around measuring the overloading capacity of the Combined Charging System (CCS-2). There are two tests performed one at 350A AC and the second one at 300A AC. When the test current is applied, the temperature will rise. The rated current is used until the temperature does not cross the limit and time is also observed for the duration of overloading.

9.2 Objectives

- Determine the overloading capacity of the Combined Charging System.
- Monitor the temperature rise limit and duration of the overloading of cables.

9.3 Statement of purpose

These tests will describe the effect of currently more than rated on the current path and the CCS-2 temperature rise. In the end duration of the temperature rise of the cable will compare with the limit provided by the IEC-62196-3 Temperature rise test.

9.4 System Descriptions and Measuring Techniques

The cable setup with the thermocouples positions is explained in Figures 6.4 & 6.6. The cable description is explained in chapter section 4.5.

Three parts are considered for the temperature rise measurement. i.e., the Contact of the cable, the Inlet part, and the Connector part.

The whole setup is the same but only the charging current is different. As this is an overloading test so apply 350A AC.

9.5 Result & Discussion

9.5.1 Overloading test at 350A

The result of the temperature rises from the software as shown in table 9-1

Table 9-1:Temperature rise across the cable at 350A

Port Number	Label	Descriptions	Initial Temperature [℃]	Maximum Temperature[℃]

101	$I_{DC+,1}$	DC+ cable of the inlet connected with power supply	19.90	26.95
102	$I_{DC-,1}$	DC- a cable of the inlet connected with the power supply	20.08	24.15
103	$I_{DC+,2}$	DC+ cable of the inlet part	19.80	47.37
104	$I_{DC-,2}$	DC- cable of the inlet part	19.88	35.44
107	$I_{DC+,3}$	DC+ cable of the inlet near to the contact	20.11	78.77
108	$I_{DC-,3}$	DC- cable of the inlet	20.45	84.55
112	Contact_1	Cable contact	20.32	36.60
113	Contact_2	Cable Contact	21.54	27.86
302	$C_{R,1}$	A red cable of the connector part near the Contact	18.92	75.39
303	$C_{B,1}$	Black cable of the connector part near the Contact	19.05	64.79
305	$C_{R,2}$	Red cable of the connector	19.28	58.28
306	$C_{B,2}$	Black cable of the connector	19.39	60.69
308	$C_{R,3}$	A red cable of the connector	19.65	56.27

310	$C_{B,3}$	Black cable of the connector	19.69	67.60
311	$C_{R,4}$	The red cable of the connector	19.87	57.85
314	$C_{B,4}$	Black cable of the connector	19.85	52.58
315	$C_{R,5}$	Red cable of the connector	19.35	54.29
316	$C_{B,5}$	Black Cable of the connector	19.36	53.16

9.6 Temperature rise

During this overloading, the test temperature rises very fastly and reaches the maximum limit within 23 minutes. The temperature on both sides of the contact like on the connector and inlet part rises very quickly as compared to the other parts of the cable. The power supply is start to decrease when the temperature of the inlet near the cable contact crosses 80℃. As from the section, 6.2.3 thermocouples wires insert into the DC contact and then close the connector with the inlet. This is the only possible solution to measure the temperature of the contact. But, there is the possibility of error because the thermocouples measure where two-wire connect. Thermocouples are mounted on the inlet and connector as close as to the contact. So, connector and inlet temperature are used as a reference and act according to it. As in the case, the temperature of the inlet is crossed 80 ℃ then the charging current is decreased, and stop the charging current after 1 or 2 minutes. To better understand the temperature, the data is plotted using MATLAB and Excel.

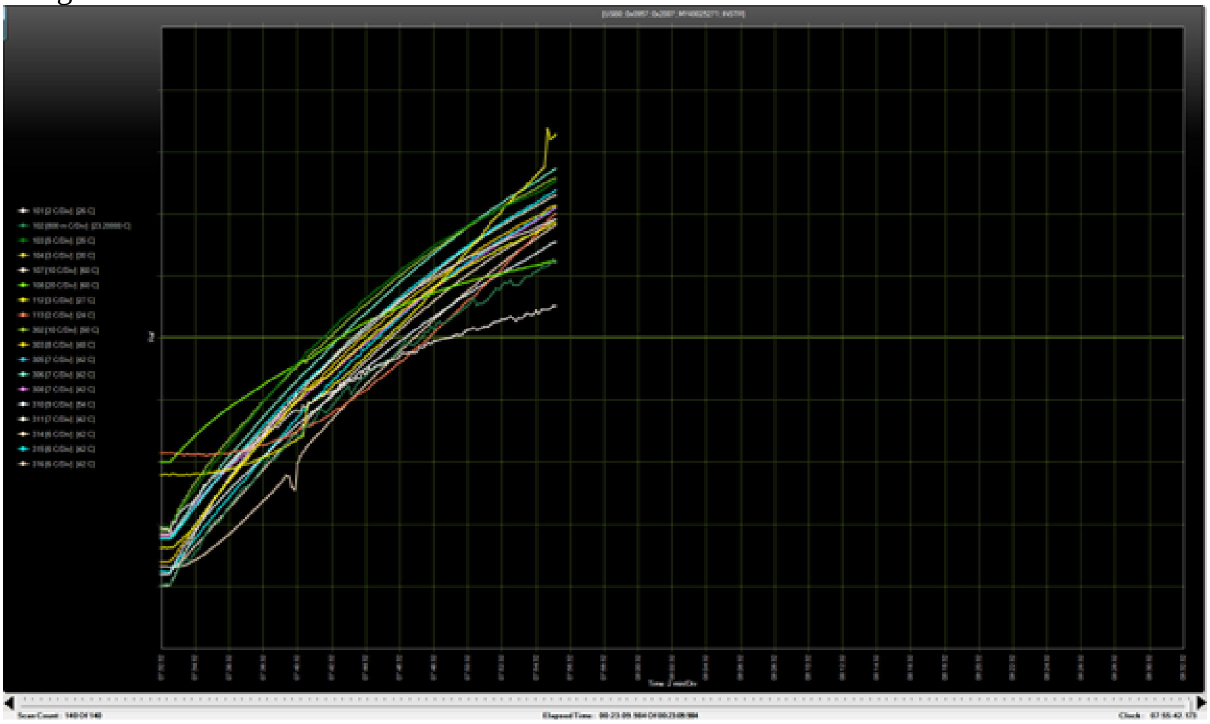

Figure 9-1:Temperature rise graph from Agilent software at 350A

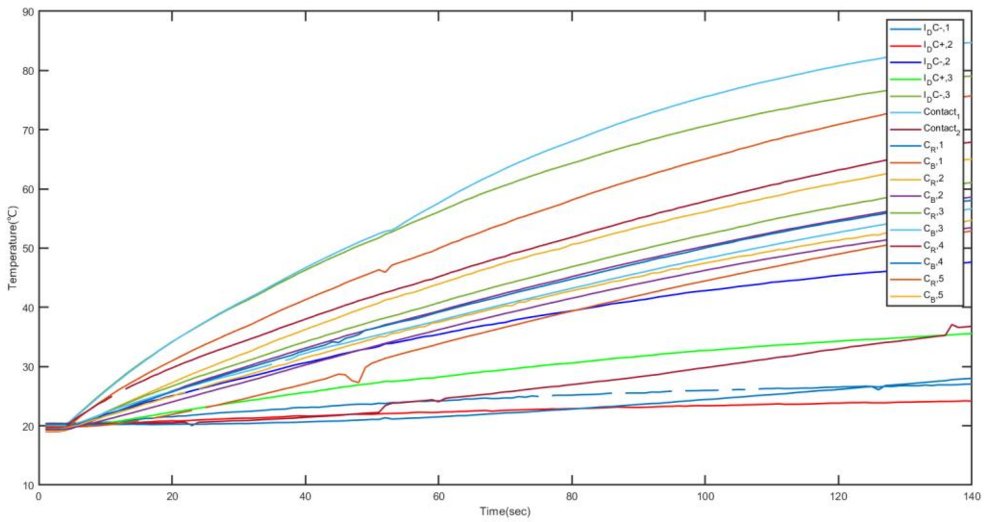

Figure 9-2:Temperature rise graph using MATLAB at 350A

9.7 Discussion

The bar is explaining the data in a good way and is easily understandable. The charging supply current decrease and stops when the temperature value crosses the IEC limit. A flow of large current in the cable beyond the limit of current is called overloading. Overloading is the cause of producing a lot of heat in the cable, Cable contact. As a result, a large amount of heating produces a fire in the cable. Continuously overloading the cable reduces the life span of the cable.

As already mention that inlet and connector temperature values as a reference because there is the possibility of error in the contact temperature monitoring. So, when the temperature of the

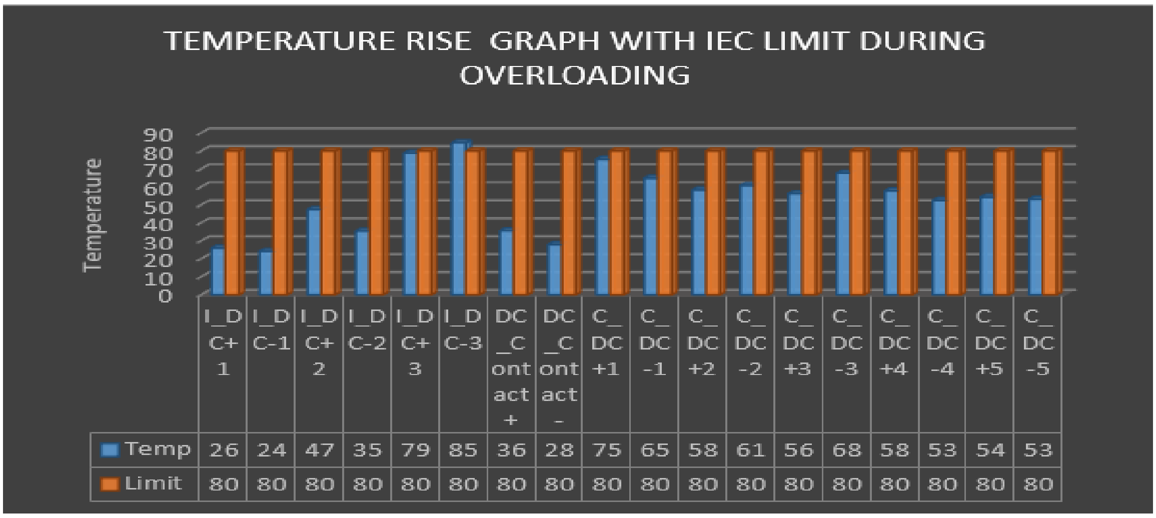

Figure 9-3:Temperature rise of cable with IEC limit during overloading current of 350A

Figure 9-4:Temperature graph from Agilent software during overloadingFigure 9-3:Temperature rise of cable with IEC limit during overloading current of 350A

inlet part crosses 80℃ then the power supply is switched off. From the bar graph, only the temperature across the contact is increased remarkably as compared to the other parts of the cable. This whole test takes 23 minutes to cross the limit.

From the above, it is clear that CCS-2 cables take 23 minutes to cross the limit of IEC temperature in the overloading test. So during the charging of the battery in the emission-free construction site the charging cable cab be overloaded for 23 minutes at 300A.

9.8 Temperature rise test at 300A overloaded current

Every construction site uses different construction machinery according to the requirement and every machinery has different specifications like different input power, output power, voltage, and current. So, one overloading test is performed to check the overloading capacity of the CCS-2 charging cable. The same setup is used to perform but change the supply current and this test is performed at 300A AC. The main purpose of this test is to check the time of overloading.

9.8.1 System Descriptions and Measuring Techniques

The same setup is used, and the same position of thermocouples is described in figures 6.4 & 6.6. Only the supply current is different and this time the supply current is 300A AC.

9.9 Result & Discussion

9.9.1 Overloading test

The result of the temperature rises from the software as shown in table 9.2

Table 9-2:Temperature rise during overloading current of 300A

Port Number	Label	Descriptions	Initial Temperature [℃]	Maximum Temperature[℃]
101	$I_{DC+,1}$	DC+ cable of the inlet connected with power supply	21.04	28.50
102	$I_{DC-,1}$	DC- a cable of the inlet connected with the power supply	21.26	26.07
103	$I_{DC+,2}$	DC+ cable of the inlet part	20.80	46.06
104	$I_{DC-,2}$	DC- cable of the inlet part	20.93	46.02
107	$I_{DC+,3}$	DC+ cable of the inlet near the contact	21.19	80.25
108	$I_{DC-,3}$	DC- cable of the inlet	21.35	78.86
112	Contact_1	Cable contact	21.85	41.97
113	Contact_2	Cable Contact	21.55	38.89
302	$C_{R,1}$	A red cable of the connector part near the Contact	19.99	80.32
303	$C_{B,1}$	Black cable of the connector part near the Contact	20.13	80.23

305	$C_{R,2}$	Red cable of the connector	20.32	62.61
306	$C_{B,2}$	Black cable of the connector	20.48	65.58
308	$C_{R,3}$	Red cable of the connector	20.59	62.98
310	$C_{B,3}$	Black cable of the connector	20.66	73.37
311	$C_{R,4}$	Red cable of the connector	20.86	61.17
314	$C_{B,4}$	Black cable of the connector	20.83	59.78
315	$C_{R,5}$	Red cable of the connector	20.67	60.68
316	$C_{B,5}$	Black Cable of the connector	20.66	59.29

9.10 Temperature rise

During this overloading, the temperature rises and reaches the maximum limit within 45 minutes. Same as the previous test the temperature on both sides of the contact like on the connector and inlet part rises very quickly as compared to the other parts of the cable. The power supply is turned off when the temperature across the cable reaches 80℃. As same as there is the possibility of error in the measurement of contact temperature due to thermocouples

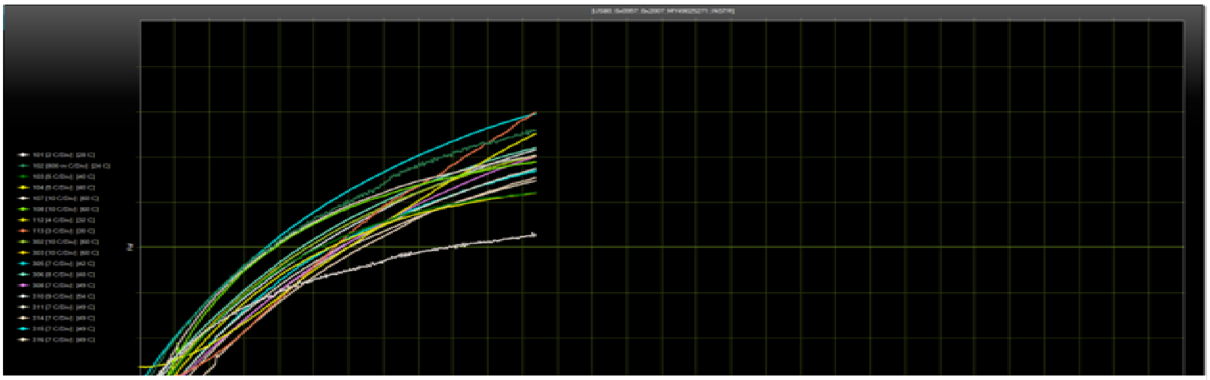

Figure 9-4:Temperature graph from Agilent software during overloading current of 300A

Figure 9-5:Temperature rise using MATLAB during overloadingFigure 9-4:Temperature graph from Agilent software during overloading current of 300A wires. The figure 9.4 shows a graph from the Agilent software. To better understand the data is plotted using MATLAB and Excel as shown in 9.5.

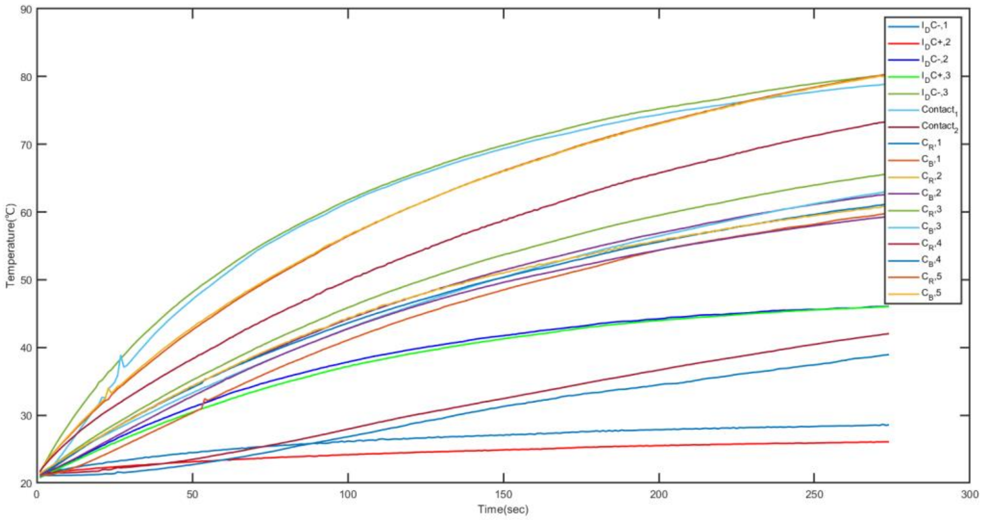

Figure 9-5:Temperature rise using MATLAB during overloading current of 300A

Figure 9-6: Temperature rise with IEC limit during overloadingFigure 9-5:Temperature rise using MATLAB during overloading current of 300A

Bar graph 9.6 shows the temperature rise of the overloading test. It can be seen that the temperature near the cable contact on both sides of the inlet and connector rises very fast and reach the IEC limit. This whole test took 45 minutes for overloading the cable. So it means that at the construction site the charging cables can be overloaded for 45 minutes at 300A.

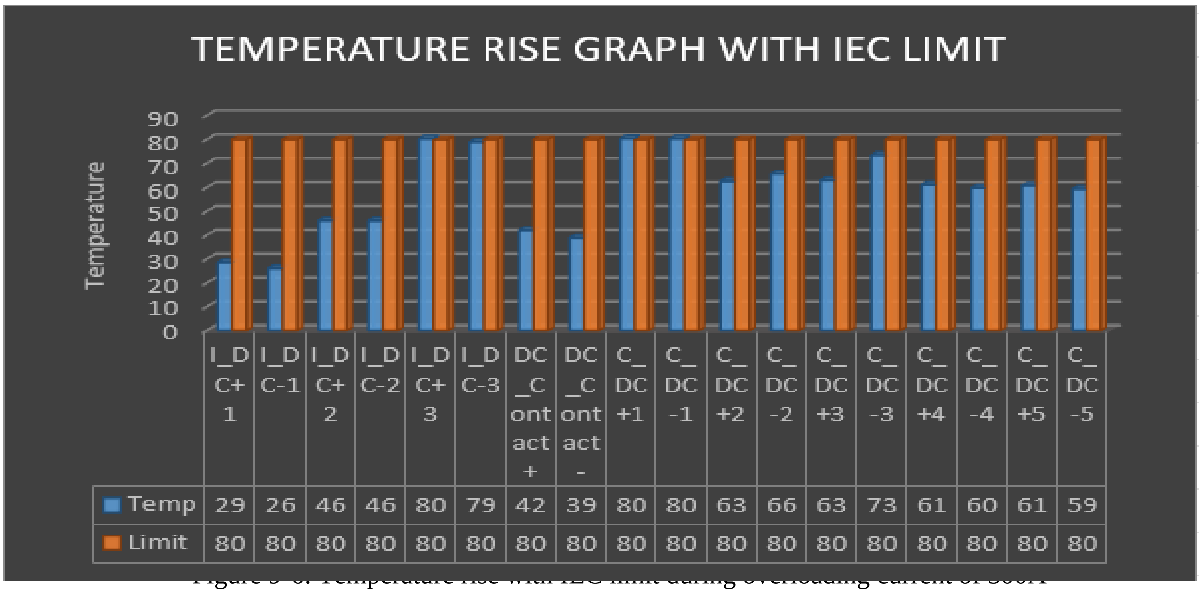

Figure 4-6:Skin depth of conductor materials for different frequencies at room temperature.Figure 9-6: Temperature rise with IEC limit during overloading current of 300A

10 Conclusion

The ability to provide extremely high electrical current over a charging wire is important to the achievement of electric vehicle adoption (EVs). High current delivery is associated with several thermal issues coming from the requirement to remove massive amounts of heat from the cable. The main goal of this thesis is to check the thermal overloading of the fast CSS-2 charging cable and based on the performed experiments proposed a charging model to avoid the thermal overloading of the charging cable on the Construction site.

First, DC Resistance Test was performed to check the quality of the cable, and cable fracture, and help to find power loss in the form of heat. So, comparing the expected and measured values of resistivity from the DC resistance test assured that the quality of the cable meets the standard and there is no fracture in the cable. Also, due to the direct relation between Resistance and heat. Now power loss($P=I^2R$) can be calculated while charging the Mobile battery on the construction site. More heat will be generated if the resistance value of the cable is increased.

A temperature rise test was performed to evaluate the performance of the CCS-2 charging cable. The temperature rise test took approximately 3 hours to reach the steady-state on the rated 250A AC. During this test, not a single part or contact of the cable crosses the IEC temperature limit. The maximum thermal time noted for the cable contact is approximately 50 minutes. During this test conduction, convection, and radiation phenomena occur and heat is flowing along the cable. Due to the conduction heat is moved from the conductor surface to the insulation and then due to convection and radiation heat is flowing from the cable surface to the surrounding environment.

The overloading test was the third test performed to check the overloading capacity of the CCS-2 charging cable.CCS-2 cable took 23 minutes to cross the limit IEC temperature limit when supplied the 350 A AC. During the overloading a lot of heat was produced across the cable, and cable contact which can damage the aging material of the cable. During this test, proper attention was needed and made sure that the temperature do not cross the IEC limit. So, from this test, batteries can be charged for 23 minutes in the case of overloading on the construction site while applying a 350A charging current.

A different variety of construction machinery is used on a typical construction site. So one more overloading was performed but at this time supplied current was 300A AC instead of 350A AC. This test took approximately 45 minutes to overload. During this test, heat is released and the temperature reaches the IEC limit. So from this test, it is clear that batteries can be charged for 45 minutes in the case of overloading on the construction site when supplying current 300A AC.

In conclusion, thermal characteristics of the CCS-2 are analyzed, and keep the test results Infront during the charging on the construction site. These results help to avoid the CCS-2 cable from thermal overloading. The actual plan is to charge the batteries during the lunch break for 30 minutes. So from the overloading tests, it is concluded that the cable can tolerate approximately 330-335A charging current for 30 minutes. As these results depend upon the ambient temperature so if the ambient temperature is changed then overloading time also changed. After taking care of these measurements then works on the construction site will not be disturbed by CCS-2 charging and will complete within the desired time. This is one of the great steps toward the Emission-free construction if everything runs smoothly, Fastly and fast charging CCS-2 cable helps to charge the batteries without thermal overloading.

References

[1] ‘Sonya Sikra, Author at GoContractor - Page 4 of 11’, *GoContractor*. https://gocontractor.com/blog/author/ssikra/ (accessed Apr. 22, 2022).

[2] ‘Emissions from Heat’, p. 12.

[3] O. US EPA, ‘Sources of Greenhouse Gas Emissions’, Dec. 29, 2015. https://www.epa.gov/ghgemissions/sources-greenhouse-gas-emissions (accessed May 13, 2022).

[4] ‘Veileder-Utslippsfrie-byggeplasser-ENG.pdf’. Accessed: Apr. 22, 2022. [Online]. Available: https://www.klimaoslo.no/wp-content/uploads/sites/88/2018/06/Veileder-Utslippsfrie-byggeplasser-ENG.pdf

[5] Anders Berger, Elisha Thapa, and Hamid Reza Mohajeri, ‘Voltage Stability Simulation of Highcapacity Charging Platform for Emission Free Construction Sites’, FM4017 Project, 201 MP-11-21.

[6] A. Hove and D. Sandalow, ‘ELECTRIC VEHICLE CHARGING IN CHINA AND THE UNITED STATES’, p. 88.

[7] D. Enescu, P. Colella, and A. Russo, ‘Thermal Assessment of Power Cables and Impacts on Cable Current Rating: An Overview’, *Energies*, vol. 13, no. 20, Art. no. 20, Jan. 2020, doi: 10.3390/en13205319.

[8] S. Czapp, S. Szultka, and A. Tomaszewski, ‘CFD-based evaluation of current-carrying capacity of power cables installed in free air’, in *2017 18th International Scientific Conference on Electric Power Engineering (EPE)*, May 2017, pp. 1–6. doi: 10.1109/EPE.2017.7967271.

[9] A. Sedaghat and F. De Leon, ‘Thermal analysis of power cables in free air: Evaluation and improvement of the IEC standard ampacity calculations’, *IEEE Trans. Power Deliv.*, vol. 29, no. 5, pp. 2306–2314, Oct. 2014, doi: 10.1109/TPWRD.2013.2296912.

[10] ‘C40_Annual_Report_2020_vMay2021_lightfile.pdf’. Accessed: Apr. 22, 2022. [Online]. Available: https://www.c40.org/wp-content/uploads/2021/11/C40_Annual_Report_2020_vMay2021_lightfile.pdf

[11] ‘Combined_Charging_System_1_0_Specification_V1_2_1.pdf’. Accessed: Mar. 10, 2022. [Online]. Available: https://tesla.o.auroraobjects.eu/Combined_Charging_System_1_0_Specification_V1_2_1.pdf

[12] ‘Combined Charging System’, *Wikipedia*. Apr. 22, 2022. Accessed: Apr. 22, 2022. [Online]. Available: https://en.wikipedia.org/w/index.php?title=Combined_Charging_System&oldid=1084018505

[13] Ç. DeriCiOğlu, E. YiRiK, E. Ünal, M. U. Cuma, B. Onur, and M. Tümay, ‘A REVIEW OF CHARGING TECHNOLOGIES FOR COMMERCIAL ELECTRIC VEHICLES’, *Int. J. Adv. Automot. Technol.*, 2018, doi: 10.15659/ijaat.18.01.892.

[14] S. Habib, M. Khan, F. Abbas, and H. Tang, ‘Assessment of electric vehicles concerning impacts, charging infrastructure with unidirectional and bidirectional chargers, and power flow comparisons’, *Int. J. Energy Res.*, vol. 42, Oct. 2017, doi: 10.1002/er.4033.

[15] A. Ahmad, Z. A. Khan, M. Saad Alam, and S. Khateeb, ‘A Review of the Electric Vehicle Charging Techniques, Standards, Progression and Evolution of EV Technologies in Germany’, *Smart Sci.*, vol. 6, no. 1, pp. 36–53, Jan. 2018, doi: 10.1080/23080477.2017.1420132.

[16] ‘SAE J1772’, *Wikipedia*. May 02, 2022. Accessed: May 13, 2022. [Online]. Available: https://en.wikipedia.org/w/index.php?title=SAE_J1772&oldid=1085796838

[17] ‘Review of static and dynamic wireless electric vehicle charging system | Elsevier Enhanced Reader’. https://reader.elsevier.com/reader/sd/pii/S221509861830154X?token=49FA32794FCB99F77737FBD0551A886E65164B968A8BE13D74F3E63C5C0BB9C8DBE98FAC5E0B681E43A218258D2C04BA&originRegion=eu-west-1&originCreation=20220209140803 (accessed Feb. 09, 2022).

[18] ‘IEC 61851-1:2017 - Electric vehicle conductive charging system - Part 1: General requirements’, *iTeh Standards Store*. https://standards.iteh.ai/catalog/standards/iec/c472de67-e272-4734-9103-cf9f4725c597/iec-61851-1-2017 (accessed Apr. 22, 2022).

[19] A. Bahrami, *EV Charging Definitions, Modes, Levels, Communication Protocols and Applied Standards*. 2020. doi: 10.13140/RG.2.2.15844.53123/11.

[20] T. Donateo, *Hybrid Electric Vehicles*. 2017.

[21] ‘High Power – Chademo Association’. https://www.chademo.com/technology/high-power/ (accessed Feb. 22, 2022).

[22] ‘Combined Charging System’, *Wikipedia*. Apr. 22, 2022. Accessed: May 13, 2022. [Online]. Available: https://en.wikipedia.org/w/index.php?title=Combined_Charging_System&oldid=1084018505

[23] ‘Combined_Charging_System_1_0_Specification_V1_2_1.pdf’. Accessed: Apr. 13, 2022. [Online]. Available: https://tesla.o.auroraobjects.eu/Combined_Charging_System_1_0_Specification_V1_2_1.pdf

[24] ‘Solutions for E-Mobility’, p. 40.

[25] ‘PHOENIX CONTACT | Combined Charging System (CCS)’. https://www.phoenixcontact.com/online/portal/pi?1dmy&urile=wcm:path:/pien/web/main/products/subcategory_pages/Charging_cables_and_charging_sockets_P-29-03/3f34965c-f842-4adc-a9f6-28126dc0a51a/3f34965c-f842-4adc-a9f6-28126dc0a51a (accessed Mar. 21, 2022).

[26] ‘Boylestad, Introductory Circuit Analysis, Global Edition, 13th Edition | Pearson’. https://www.pearson.com/uk/educators/higher-education-educators/program/Boylestad-Introductory-Circuit-Analysis-Global-Edition-13th-Edition/PGM1093740.html (accessed May 13, 2022).

[27] E.-E. E. Portal, ‘Copper Busbar Jointing Methods’, *EEP - Electrical Engineering Portal*, Jun. 17, 2015. https://electrical-engineering-portal.com/5-copper-busbar-jointing-methods (accessed May 13, 2022).

[28] R. A. Serway, *Principles of physics*, 2nd ed. Fort Worth: Saunders College Pub., 1998.

[29] ‘IEC 60287-1-1:2006 | IEC Webstore’. https://webstore.iec.ch/publication/1265 (accessed May 13, 2022).

[30] ‘4-wire method resistance measurement - Google Search’. https://www.google.com/search?q=4-wire+method+resistance+measurement&sxsrf=ALiCzsahOBHjrO6u8yqKc6zlFWu4m6O0ig:1652447514312&source=lnms&tbm=isch&sa=X&ved=2ahUKEwjgw-bYxtz3AhWwtYsKHX1LD4cQ_AUoAXoECAEQAw&biw=1536&bih=656&dpr=1.25#imgrc=zUl-4A9aEbusSM (accessed May 13, 2022).

[31] ‘conductor-Resistance.pdf’. Accessed: May 13, 2022. [Online]. Available: https://www.siechem.com/wp-content/uploads/2017/02/conductor-Resistance.pdf

[32] H. Kwak, ‘Thermal capacity and loading assessment for 24 kV XLPE-insulated cables in air’, 2021, Accessed: May 13, 2022. [Online]. Available: https://openarchive.usn.no/usn-xmlui/handle/11250/2773852

[33] ‘Boylestad, Introductory Circuit Analysis, Global Edition, 13th Edition | Pearson’. https://www.pearson.com/uk/educators/higher-education-educators/program/Boylestad-Introductory-Circuit-Analysis-Global-Edition-13th-Edition/PGM1093740.html (accessed May 13, 2022).

[34] ‘E. Fjeld and W. Rondeel, Physics of Electrical Power Engineering.’

[35] I. Garniwa and A. Burhani, ‘Thermal Incremental And Time Constant Analysis On 20 Kv XLPE Cable With Current Vary’, in *2006 IEEE 8th International Conference on Properties applications of Dielectric Materials*, Jun. 2006, pp. 566–569. doi: 10.1109/ICPADM.2006.284241.

[36] S. Mo, J. Zhang, D. Liang, and H. Chen, ‘Study on Pyrolysis Characteristics of Cross-linked Polyethylene Material Cable’, *Procedia Eng.*, vol. 52, pp. 588–592, Dec. 2013, doi: 10.1016/j.proeng.2013.02.190.

[37] F. P. Incropera and F. P. Incropera, Eds., *Fundamentals of heat and mass transfer*, 6th ed. Hoboken, NJ: John Wiley, 2007.

[38] ‘Numerical modeling of the thermal behavior of XLPE Power Cable’, *EMWorks*. https://www.emworks.com/application/numerical-modeling-of-the-thermal-behavior-of-xlpe-power-cable (accessed May 13, 2022).

[39] G. Wypych, *Handbook of Polymers*. Elsevier, 2022.

[40] ‘Specific Heat of common Substances’. https://www.engineeringtoolbox.com/specific-heat-capacity-d_391.html (accessed May 13, 2022).

[41] H. Gremmel, ABB-Calor-Emag-Schaltanlagen AG, and ABB-Calor-Emag-Mittelspannung GmbH, Eds., *Switchgear manual*, 10., rev. Ed. Berlin: Cornelsen, 2001.

[42] ‘Electrical Engineer’s Reference Book - 16th Edition’. https://www.elsevier.com/books/electrical-engineers-reference-book/laughton/978-0-7506-4637-6 (accessed May 13, 2022).

[43] U. Hauck and M. Ludwig, ‘Thermal Modeling for High Power Charging (HPC) of Electric Vehicles’, in *Electrified Mobility 2019*, J. Liebl, Ed. Wiesbaden: Springer Fachmedien Wiesbaden, 2022, pp. 155–166. doi: 10.1007/978-3-658-32471-1_14.

[44] ‘Primary Current Injection Testers’. http://www.hilkar.com/highcurrentinjectiontestsets.html (accessed May 07, 2022).

[45] ‘eCARS2x_Lecture_Notes_L3-3.pdf’. Accessed: Feb. 10, 2022. [Online]. Available: https://ocw.tudelft.nl/wp-content/uploads/eCARS2x_Lecture_Notes_L3-3.pdf

[46] ‘Vehicle charging inlet - CHARX T2HBI12-3AC32DC250-2,0M2 - 1162095 | Phoenix Contact’. https://www.phoenixcontact.com/en-za/products/vehicle-charging-inlet-charx-t2hbi12-3ac32dc250-20m2-1162095 (accessed Apr. 22, 2022).

[47] Q. Wei, H. Chen, J. Wang, and X. Li, ‘Research on Temperature Rise Performance of EV Charging Coupler’, *J. Phys. Conf. Ser.*, vol. 1626, no. 1, p. 012039, Oct. 2020, doi: 10.1088/1742-6596/1626/1/012039.

11 Appendix

Title : Emission free construction sites – thermal overloading of the charging system

USN supervisor: Elin Fjeld

External partner: Skagerak Energi

Task background:

Construction activities in Norway accounted for direct emissions of approximately 2 million tons of CO2 in 2019 (SSB). Electrification of the sector is desirable to reduce these emissions. To realize a fossil-free construction site, access to sufficient electrical energy and power is required. On many of the construction sites, however, the access electric power from the power grid is limited. Expanding the power grid on these sites in connection with the construction process is often not very appropriate, as there is often no need for this upgrade after the construction process has been completed. To meet the electrical energy needs during construction without upgrading the local power grid, battery technology might be a solution. Skagerak Energi has gained funding from Enova for a research project where mobile battery containers are used in the electrification of construction sites. The idea is to charge batteries at a location where the grid has good capacity. Fully charged batteries are then driven from the charging station to the relevant construction site to supply battery-powered construction machines. When the battery is discharged, the empty battery is driven to the nearest charging station, and a new, fully charged battery is driven to the construction site. The study will include a pilot project with four mobile battery containers and two charging stations. University of South-Eastern Norway is a research partner in the project and will contribute to the planning of the pilot as well as analysis of data from the pilot project. The charging system (including charging cables) has a certain continuous loading capacity. However, it can be overloaded for shorter times to facilitate fast charging e.g. during lunch break as long as the temperature is kept within the limits.

Task description:

The student should

- Make an overview of the charging system.
- Identify what equipment is the limiting factor when it comes to thermal overloading.
- Study theory regarding thermal dimensioning of relevant equipment.
- Search the literature for studies on temporary overloading of relevant equipment.
- Investigate what temperature limits apply.
- Make a test set-up in the high current laboratory for thermal testing of charging cables.
- Use the tests to make an initial, simplified thermal model of the charging cables.

Student category: EPE

Is the task suitable for online students (not present at the campus)? No

Practical arrangements:
Skagerak will help provide the charging cables for the tests.
Supervision:
As a general rule, the student is entitled to 15-20 hours of supervision. This includes necessary time for the supervisor to prepare for supervision meetings (reading material to be discussed, etc).
Signatures:
Supervisor (date and signature):

Student (write clearly in all capitalized letters):

MUHAMMAD AKHLAQ

Student (date and signature):

13-May-2022.